Nuclear Physics B257 [FS14] (1985) 799–858

THE PATH DECOMPOSITION EXPANSION AND MULTIDIMENSIONAL TUNNELING

Assa AUERBACH and S. KIVELSON

Department of Physics, State University of New York at Stony Brook, New York, USA

Received 7 March 1985

This paper consists of two main topics.

(i) The path decomposition expansion: a new path integral technique which allows us to break configuration space into disjoint regions and express the dynamics of the full system in terms of its parts.

(ii) The application of the PDX and semiclassical methods for solving quantum-mechanical tunneling problems in multidimensions. The result is a conceptually simple, computationally straightforward method for calculating tunneling effects in complicated multidimensional potentials, even in cases where the nature of the states in the classically allowed regions is nontrivial. Algorithms for computing tunneling effects in general classes of problems are obtained.

In addition, we present the detailed solutions to three model problems of a tunneling coordinate coupled to a phonon. This enables us to define various well-controlled approximation schemes, which help to reduce the dimensions of complicated tunneling calculations in real physical systems.

1. Overall introduction

There are many situations in quantum mechanics in which the configuration space breaks up naturally into different regions, in each of which different approximations are useful for solving Schrödinger's equation. While the nature of the quantum states is largely locally determined, they also depend on certain global properties of the potential and boundary conditions. Thus there is a need for a "patching up" scheme, which enables us to use the partial information about each isolated region of space to obtain solutions of the full problem in the full configuration space. This is our motivation for introducing the path decomposition expansion (PDX), which is a new technique in path integration [1].

If we consider a multidimensional configuration space which is divided into two (or more) distinct regions by a surface (or surfaces), the PDX allows us to express the full time evolution operator of the system as a time convolution and surface integrations of products of restricted Green functions, each of which involves the sum over paths that are limited to different regions of space. We believe that the PDX will prove to be useful for a variety of applications since it permits us to use

different approximation schemes to evaluate each of the restricted Green functions. This is certainly the case in the tunneling problems where configuration space breaks up into classically allowed regions ("wells") and classically forbidden regions ("barriers"). Since the PDX could be applied to a wider class of problems we chose to present the formalism in a separate self-contained part (sect. 2).

In the following parts (sects. 3 and 4) we demonstrate the usefulness of the PDX formalism for solving multidimensional tunneling problems. In particular, we show that even for tunneling problems involving rather complicated nonseparable potentials, the qualitative behavior is readily inferred and *quantitative* solutions can be obtained from knowledge of the classical dynamics. In cases where the classical dynamics cannot be solved in closed analytic form, numerical solutions, which are relatively easy to obtain, can be used to calculate the quantum mechanical tunneling rates. Sect. 4 of this paper consists of a series of solutions to model problems. These problems are of generic interest since they exhibit features contained in many tunneling systems. In particular the separation of time scales and renormalization effects, which are discussed qualitatively in sect. 3, are here demonstrated in detail.

The paper is organized in the following fashion: each part is independent, and starts with a separate introduction in which the problems to be studied are defined, the approximation schemes motivated, and the results are described.

Sect. 2 consists of exact results concerning the PDX for path integrals. The principal results derived in this part are:

(i) The single surface decomposition formula, with a discussion of the analytic structure of the restricted Green function.

(ii) The generalization of the PDX to multiple decomposition surfaces.

(iii) The proof of an exact new representation of the full hamiltonian in the direct sum space of the restricted states.

In sect. 3, a method for solving multidimensional tunneling problems is described which is based on the PDX and the semiclassical evaluation of the restricted Green function in the classically forbidden region. Loosely speaking, this is a multidimensional generalization of the WKB method (see e.g. [2]), in which the PDX plays the role of the connection formula. This is the principal result of sect. 3. In particular we show that the low-lying states of a system consisting of two or more wells can be represented by a truncated hamiltonian in which the wells of the original tunneling problem are replaced by a well-defined set of discrete states, with calculable tunneling matrix elements connecting the states of different wells. It should be stressed, however, that in general the nature of the discrete states and the values of the matrix elements cannot be derived by truncating a one-dimensional hamiltonian; they involve the solution of the multidimensional tunneling problem as is emphasized in the second half of sect. 3. There we discuss how a generic physical problem can be reduced to a sufficiently simple form that it can be treated sensibly by our methods. Thus we consider the question: which degrees of freedom must be *explicitly* included in the tunneling calculation? We find that if there is a separation

of time scales then it is possible to identify "fast" modes which can be treated in the adiabatic approximation (they simply renormalize the effective mass and potential of the tunneling coordinate [3]), and "slow" modes which can be kept as fixed (frozen) parameters in the tunneling calculation and considered as residual interactions in the truncated hamiltonian. Only those "important" degrees of freedom with characteristic frequencies in a limited range need be considered explicitly!

Sect. 3 concludes with a summary section written in a "cook-book" fashion. It outlines a strategy for solving a tunneling problem in a general system with many coupled degrees of freedom.

Sect. 4 is an extensive treatment of the ground state tunnel splitting of the quartic double well which is coupled to a harmonic oscillator (phonon). Three couplings are discussed: Linear in both the tunneling and phonon coordinates ("linear"), quadratic in the tunneling and linear in the phonon coordinate, ("gated"), and quadratic in both coordinates ("squeezed"). By comparing the results of the PDX computation to different approximations we are able to chart the parameter spaces of these problems and bound the regions of validity of the approximation schemes (see figs. 12 and 13). The squeezed double well exhibits the remarkable phenomenon of quantum (dynamical) induced barrier formation, in which the transverse quantum fluctuations account for a sizeable renormalization of the barrier height and thus the tunneling rates in such a problem have an anomalous dependence on the mass.

The paper is concluded with a summary and discussion section. Here, we briefly compare the present work with some previous work along similar lines. Then we speculate about the outlook for further applications of the PDX especially to semiclassical methods in infinite degrees of freedom (field theoretical) models.

Finally, we include a series of appendices (A-D) which provide some technical details and simple examples that were omitted from the main text but may be useful to the reader who wishes to familiarize himself with this technique.

2. The path decomposition expansion

2.1. INTRODUCTION

The Feynman path integral formulation of quantum mechanics allows us to express the Green function $K(\boldsymbol{x}_1, \boldsymbol{x}_2, T)$ for Schrödinger's equation as a sum over all continuous paths from point $\boldsymbol{x}_1$ to point $\boldsymbol{x}_2$ in an N-dimensional configuration space $\mathcal{Q}$. (For a comprehensive review refs [4, 5] are suggested.) The PDX is based on the observation that if configuration space is divided into two distinct regions by an $(N-1)$-dimensional surface, Σ, and if $\boldsymbol{x}_1$ is in one region (which we call the "inside") and $\boldsymbol{x}_2$ is in the other ("outside"), then any path from the one point to the other must cross the surface Σ at least once. (Of course the typical path will cross Σ many times, see fig. 1). We can therefore divide every path into two pieces according to the last crossing time t: a piece that goes from $\boldsymbol{x}_1$ to the crossing point $\boldsymbol{x}_\sigma$ on Σ in

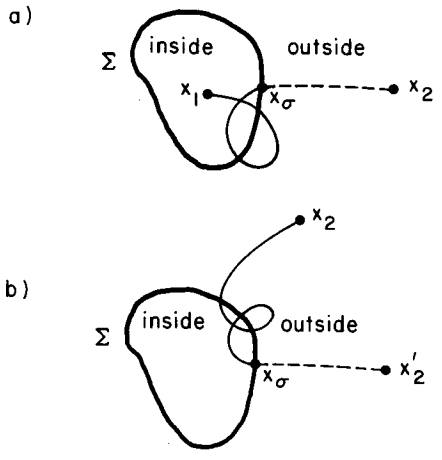

Fig. 1. Single surface decomposition. Schematic representation of the path decomposition in Eqs. (2.17) and (b) (2.18) at a surface Σ. (a) A typical path in $G(x_1, x_2, E)$ with x_1 inside and x_2 outside Σ. (b) A typical path in $G(x_2, x_2', E) - G^r(x_2, x_2', E)$ with both x_2 and x_2' outside Σ.

time t, and a piece that in the remaining time $T-t$ goes directly from x_σ to x_2 without ever crossing Σ again. This is what is meant by path decomposition. It results in an expression (eq. 2.13) which equates the full Green function to a convolution over crossing times t and a surface integration dx_σ of the full Green function $K(x_1, x_\sigma, t)$ and a restricted Green function $K^r(x_\sigma, x_2, T-t)$ which is equal to the sum over all paths from x_σ to x_2 which do not cross Σ.

We derive this result in two ways: the first derivation is in terms of the discrete time step version of the path integral for the Green function analytically continued to imaginary time. Here a genuine (Wiener) measure exists, and we are on firm mathematical grounds. In a second, more intuitive, approach, we describe the PDX as a transformation of integration variables in path space, and the functional jacobian which is required leads to the same result. It is important to understand the properties of the restricted Green function G^r which is the Laplace transform of K^r. We show that as defined from the path integral formulation, G^r is just the usual Green function in the presence of an infinite hard wall at Σ. However it is possible to consider the decomposition formula as a Green function identity, in which case G^r can satisfy a variety of boundary conditions on Σ which are still consistent with this identity. (For examples see appendix A.)

In subsect. 2.2 the single surface PDX is derived for the two cases: (i) the endpoints lie on either side of Σ, (ii) the endpoints are both outside Σ. In subsect. 2.3 the PDX is generalized to multiple decomposition surfaces. The full Green function is expanded as a sum over topologically distinct sets of paths, which is described by a multiple transition series that involves the different restricted Green functions. In subsect. 2.4 the series is summed up, and we derive a new representa-

tion for the full hamiltonian in the direct sum space of the restricted eigenstates. Thus we formally break up the hamiltonian into separate hamiltonians which are coupled by energy-dependent transition matrix elements, and literally provide a construction of the full quantum system from its parts.

2.2. THE SINGLE SURFACE PDX

In this section we derive the PDX on a single closed $(N-1)$-dimensional surface Σ in the N-dimensional configuration space, $\mathcal{Q}$. The matrix elements of the Schrödinger time evolution operator between eigenstates $|x\rangle$ of the position operator is the Green function, K, also called the "propagator", which can be expressed in terms of a Feynman path integral [4]:

$$K(x_1, x_2, T) = \int_{x(0)=x_1}^{x(T)=x_2} \mathcal{D}[x] \exp\left(i \frac{\mathcal{S}[x]}{\hbar} \right), \tag{2.1}$$

where x is a vector in $\mathcal{Q}$, $\mathcal{S}$ is the action functional

$$\mathcal{S}[x] = \int_0^T \mathrm{d}t \left[\tfrac{1}{2} m \dot{x}^2 - V(x) \right], \tag{2.2}$$

m is the mass and $V(x)$ is the potential defined on $\mathcal{Q}$. In order to avoid unnecessary complications we will actually consider the (Wick-rotated) Green function of imaginary time $K(x_1, x_2, -iT)$. This entails replacing the action $\mathcal{S}$ in eq. (2.2) by the analytically continued action $\mathcal{S} \mapsto iS$ where

$$S[x] = \int_0^T \mathrm{d}t \left[\tfrac{1}{2} m \dot{x}^2 + V(x) \right]. \tag{2.3}$$

Notice that S is the action corresponding to the inverted potential. The imaginary-time Green function is a simpler quantity to deal with because its path integral representation has a well-defined measure, the Wiener measure of brownian motion paths [5]. The real-time Green function can always be obtained by analytic continuation of the imaginary time function.

Let us first treat the PDX in a one-dimensional configuration space where Σ is the single point x_σ that lies between the two points $x_0 < x_\sigma < x_T$. The path integral is defined to be the limit as the number of time steps, M, in the discrete time path integral K_M goes to infinity:

$$K(x_0, x_T, -iT) = \lim_{M \to \infty} K_M(x_0, x_T, -iT), \tag{2.4}$$

where $x_{M+1} = x_T$ and

$$K_M = \left[\frac{m}{2\pi\hbar\epsilon} \right]^{(M+1)/2} \int_{-\infty}^{\infty} \mathrm{d}x_1 \mathrm{d}x_2 \ldots \mathrm{d}x_M \exp\left[- \frac{S(0, M+1)}{\hbar} \right]. \tag{2.5a}$$

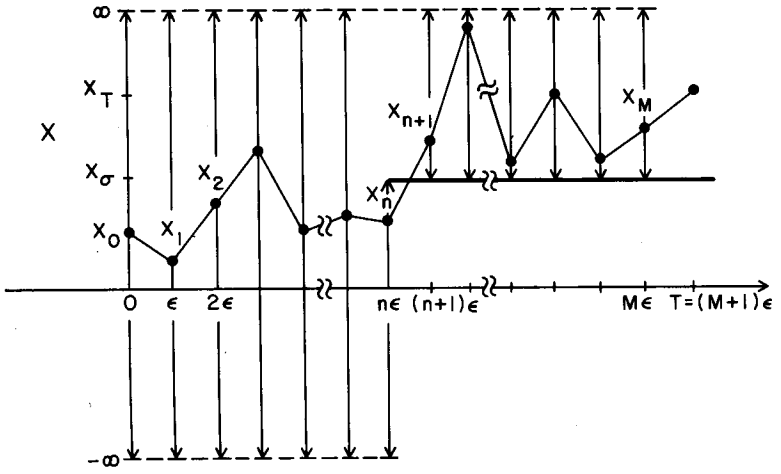

Fig. 2. A typical path in $\mathcal{P}_n$ which contributes to $K_{M,n}$. The arrows indicate the limits of integrations of x_j, $j = 1, M$ in eq. (2.6b).

Here $S(n_1, n_2)$ is the discretized version of the action

$$S(n_1, n_2) = \sum_{j=n_1}^{n_2} \left[\frac{m(x_{j+1} - x_j)^2}{2\varepsilon} + V(x_j)\varepsilon \right], \tag{2.5b}$$

K_M is the time discretized version of the path integral and $\varepsilon = T/(M+1)$ is the time step.

If we imagine connecting points x_i by straight line segments to $x_{i\pm1}$, then the M points x_i, $i = 1, M$ in eqs. (2.5) can be seen to specify a path. Since any path from x_0 to x_T must cross x_σ at least once, the paths can be grouped into $M+1$ disjoint sets $\mathcal{P}_n$, labeled by the integer $n = 0, 1, \ldots M$ so that $\mathcal{P}_n$ consists of all the paths for which the largest value of j that satisfies $x_j \leqslant x_\sigma$ is $j = n$. A typical path in $\mathcal{P}_n$ is illustrated in fig. 2. By regrouping in this fashion, K_M can be written as

$$K_M(x_0, x_T, -iT) = \sum_{n=0}^{M} K_{M,n}(x_0, x_T, -iT), \tag{2.6a}$$

where $K_{M,n}$ is the sum over all paths which are members of $\mathcal{P}_n$:

$$K_{M,n} = \left[\frac{m}{2\pi\hbar\varepsilon} \right]^{(M+1)/2} \int_{-\infty}^{\infty} \cdots \int_{-\infty}^{\infty} \mathrm{d}x_1 \mathrm{d}x_2 \ldots \mathrm{d}x_{n-1} \exp\left[-\frac{1}{\hbar} S(0, n-1) \right]$$

$$\times \int_{-\infty}^{x_\sigma} \mathrm{d}x_n \int_{x_\sigma}^{\infty} \cdots \int_{x_\sigma}^{\infty} \mathrm{d}x_{n+1} \mathrm{d}x_{n+2} \ldots \mathrm{d}x_M \exp\left[-\frac{1}{\hbar} S(n-1, M+1) \right]. \tag{2.6b}$$

Since $S(n-1, M+1)$ depends on x_{n-1}, the expression in (2.6b) cannot be written as a product of independent integrals; however we shall factorize $K_{M,n}$ using the following identity:

$$\left[\frac{m}{2\pi\hbar\varepsilon}\right]^{1/2}\exp\left[-\frac{m(x_{n+1}-x_n)^2}{2\hbar\varepsilon}\right]$$

$$=\int_0^{\varepsilon}\mathrm{d}\tau\left(\frac{m}{2\pi\hbar\tau}\right)^{1/2}\exp\left[-\frac{m(x_\sigma-x_n)^2}{2\hbar\tau}\right]$$

$$\times\frac{\hbar}{m}\frac{\partial}{\partial_x}\left[\left(\frac{m}{2\pi\hbar(\varepsilon-\tau)}\right)^{1/2}\exp\left[-\frac{m(x_{n+1}-x)^2}{2\hbar(\varepsilon-\tau)}\right]\right]_{x=x_\sigma}, \qquad (2.7)$$

which holds whenever x_σ lies between x_n and x_{n+1}. This identity can be verified by applying the Laplace convolution (Faltung) theorem, and using the Laplace transform integral

$$\int_0^{\infty}\mathrm{d}t\,\mathrm{e}^{-st}\frac{1}{\sqrt{\pi t}}\exp\left(-\frac{k^2}{4t}\right)=\frac{1}{\sqrt{s}}\exp(-k\sqrt{s}), \qquad k\geqslant 0. \qquad (2.8)$$

We use this identity in eq. (2.6b) and the symmetry of the integrand under $x_n-x_\sigma\to x_\sigma-x_n$ to extend the x_n integral to $+\infty$, (and thereby obtain a compensating factor of $\frac{1}{2}$). The result is the factorized expression for $K_{M,n}$:

$$K_{M,n}(x_0, x_T, -iT)$$

$$=\int_0^{\varepsilon}\mathrm{d}\tau K_n(x_0, x_\sigma, -i(n\varepsilon+\tau))$$

$$\times\frac{\hbar}{2m}\frac{\partial}{\partial_x}K^{\mathrm{r}}_{(M-n)}(x, x_T, -i(T-n\varepsilon-\tau))|_{x=x_\sigma}(1+\mathrm{O}(\varepsilon^{3/2})),$$

(2.9)

and K^{r}_M is defined the same way as K_M (eq. (2.5)) except that the x_j integrals have a lower bound at x_σ instead of $-\infty$. The terms in (2.9) that are indicated by the $\mathrm{O}(\varepsilon^{3/2})$ arise from the potential term in S. More specifically, in deriving (2.9) we ignored terms proportional to the gradient of $V(x)$:

$$V(x_n)\varepsilon=[V(x_n)\tau+V(x_\sigma)(\varepsilon-\tau)]-\frac{\partial}{\partial_x}V(x_n)(x_\sigma-x_n)(\varepsilon-\tau)+\cdots.$$

(2.10)

The contribution to $K_{M,n}$ from the first derivative term in (2.10) is $O(\varepsilon^{3/2})$ since the only significant contribution to the x_n integral comes from the region $(x_n - x_\sigma) \sim \varepsilon^{1/2}$. In the $M \to \infty$ limit, this term can be ignored. Moreover, in this limit $K_n \to K$, $K^{\mathrm{r}}_{M-n} \to K^{\mathrm{r}}$ and the sum over n with the integral over τ are replaced by a single integral over $t = n\varepsilon + \tau$, which results in the PDX expression for K:

$$K(x_0, x_T, -iT) = \int_0^T \mathrm{d}t\, K(x_0, x_\sigma, -it) \frac{\hbar}{2m} \frac{\partial}{\partial_x} K^{\mathrm{r}}(x, x_T, -i(T-t))\big|_{x=x_\sigma}, \tag{2.11}$$

where the restricted Green function K^{r} is

$$K^{\mathrm{r}}(x, x', -it) \equiv \int_{x(0)=x}^{x(t)=x'} \mathcal{D}^{\mathrm{r}}[x] \exp\left(-\frac{S[x]}{\hbar}\right), \tag{2.11'}$$

and $\mathcal{D}^{\mathrm{r}}[x]$ is the restricted measure which excludes any path that crosses x_σ.

Extending (2.11) to the multidimensional case is straightforward; we merely sketch the derivation. The paths can be grouped as before into disjoint sets $\mathcal{P}_n$ based on the last point $\boldsymbol{x}_n$ which is inside Σ. Since $|\boldsymbol{x}_n - \boldsymbol{x}_{n+1}| \sim \varepsilon^{1/2}$, we can treat the surface as being locally flat over the range of the $\boldsymbol{x}_n$ integration. (Again, this ignores higher-order terms in ε.) We parametrize displacements along the surface by the components $x_{\sigma,i}$, $i = 2, N$ and choose $x_{\sigma,1}$ to be along the unit vector, $\hat{\boldsymbol{n}}_1$, normal to Σ. This enables us to carry out the same decomposition as in (2.6) for the 1-coordinate. In order to factorize the expression which is analogous to (2.6b) we use an additional identity of gaussian integrals:

$$\left[\frac{m}{2\pi\hbar\varepsilon}\right]^{1/2} \exp\left[-\frac{m(x_{n+1,i} - x_{n,i})^2}{2\hbar\varepsilon}\right]$$

$$= \int_{-\infty}^{\infty} \mathrm{d}x_{\sigma,i} \left(\frac{m}{2\pi\hbar\tau}\right)^{1/2} \exp\left[-\frac{m(x_{\sigma,i} - x_{n,i})^2}{2\hbar\tau}\right] \left(\frac{m}{2\pi\hbar(\varepsilon-\tau)}\right)^{1/2}$$

$$\times \exp\left[-\frac{m(x_{n+1,i} - x_{\sigma,i})^2}{2\hbar(\varepsilon-\tau)}\right]. \tag{2.12}$$

Thus we end up with the generalization of the PDX (2.11) to multidimensions. After analytically continuing to real time we arrive at the expression

$$K(\boldsymbol{x}_0, \boldsymbol{x}_T, T) = \int_0^T \mathrm{d}t \int_\Sigma \mathrm{d}\sigma K(\boldsymbol{x}_0, \boldsymbol{x}_\sigma, t) \left(\frac{i\hbar}{2m} \hat{\boldsymbol{n}}_1 \cdot \nabla\right) K^{\mathrm{r}}(\boldsymbol{x}, \boldsymbol{x}_T, T-t)\big|_{x=x_\sigma}, \tag{2.13}$$

where $d\sigma$ denotes the integration $\prod_{i=2}^{N} dx_{\sigma,i}$, and K^r is the sum over all paths which never cross Σ. K^r is equivalent to the Green function in the presence of $V(x)$ plus an infinite potential barrier along Σ. Note that $K^r(x, x', T)$ vanishes for either x or x' on Σ.

Eq. (2.13) can be obtained as a transformation of integration variables in path space, since the resummation could be considered as a substitution of one spatial integration variable, namely $x_{\sigma,1}$, in the path integral by a time integration. If $[x_t(\tau)]_0^T$ is a path that obeys $x_t(t) = x_\sigma$, and $x_t(\tau) > x_\sigma$ for $\tau > t$, the functional jacobian $\mathcal{J}$ of the change of variables is

$$\mathcal{J}[x_t(\tau)] = \left.\frac{\delta x_t(\tau)}{\delta t}\right|_{\tau=t} = \tfrac{1}{2}[v^{\text{in}} + v^{\text{out}}], \tag{2.14}$$

where v^{in} and v^{out} are the incoming and outgoing velocities of $x(\tau)$ at the surface point. This method of defining the PDX yields a symmetric form for eq. (2.13),

$$K(x_0, x_T, T) = \int_0^T dt \int_\Sigma d\sigma K(x_0, x_\sigma, t)\left[\frac{-i\hbar}{2m}\hat{n}_1 \cdot \overline{\nabla}\right] K^r(x_\sigma, x_T, T-t)|_{x=x_\sigma}, \tag{2.15a}$$

where

$$f\overline{\nabla}g = (\nabla f)g - (\nabla g)f. \tag{2.15b}$$

Since K^r vanishes at Σ, the first term does not contribute and eqs. (2.13) and (2.15) are identical.

It is often more convenient to deal with the energy Green function G, which is the Laplace transform of K:

$$G(x_1, x_2, E) = i\int_0^\infty dt K(x_1, x_2, t) e^{i(E+i\eta)t/\hbar}, \tag{2.16}$$

where $\eta \to 0^+$ is an infinitesimal which imposes causal boundary conditions. Since the PDX involves a convolution of two Green functions, it transforms into a simple identity for the energy Green functions. Thus for any x_1 inside Σ and x_2 outside Σ:

$$G(x_1, x_2, E) = \int_\Sigma d\sigma G(x_1, x, E)\left[\frac{\hbar}{2m}\hat{n}_1 \cdot \overline{\nabla}\right] G^r(x, x_2, E)|_{x=x_\sigma}, \tag{2.17}$$

where G^r is the Laplace transform of K^r as in eq. (2.16) which also obeys vanishing (Dirichlet) boundary conditions on Σ. Since we will be using the PDX extensively in subsect. 2.3, it is useful to introduce more compact notation. We do this by expressing the PDX in operator form such that eq. (2.17) is written as

$$\langle x_1|G(E)|x_2\rangle = \langle x_1|G(E)[\Sigma]G^r(E)|x_2\rangle, \tag{2.17'}$$

where $[\Sigma]$ is the surface decomposition operator

$$[\Sigma] \equiv \lim_{x, x' \to x_\sigma} \int_\Sigma d\sigma \; |x_\sigma\rangle\langle x| \left[\frac{\hbar}{2m} \hat{n}_1 \cdot \overleftrightarrow{\nabla} \right] |x'\rangle\langle x_\sigma| \; . \tag{2.17''}$$

The second single surface PDX expression describes the case where the endpoints x_2 and x_2' are both outside the closed decomposition surface Σ. We follow the analogous steps of the previous proof and arrive at the expression

$$G(x_2, x_2', E) - G^r(x_2, x_2', E) = \langle x_2 | G[\Sigma] G^r | x_2' \rangle , \tag{2.18}$$

where G^r is the same restricted Green function as in eq. (2.17). Evidently eq. (2.18) follows from the following argument: since all paths in $G - G^r$ are the ones that necessarily cross Σ, they all have a "last crossing time" and can be decomposed at Σ in the same way as the paths contained in the previous expression, eq. (2.17). In fig. 1b a typical path in $G - G^r$ is illustrated.

The analytic structure of the energy Green function can be described by

$$G(x, x', E) = -\hbar \sum_n \frac{\psi_n^*(x) \psi_n(x')}{E - E_n + i\eta} , \tag{2.19}$$

where ψ_n and E_n are the eigenstates and their energies respectively. In a range of energies in which the spectrum consists of only normalizable states, $G(E)$ is real. When E lies in a region of continuous density of states, $\rho(E), G(E)$ has an imaginary part proportional to $\rho(E)$, and the sum in eq. (2.19) becomes an integral. Since G^r obeys different boundary conditions, it can be described analogously to eq. (2.19) but with different eigenstates and energies.

The PDX expression (eqs. (2.17), (2.18)), can be also viewed as a Green function identity that actually *defines* the restricted Green function. Using Green's theorem one can show that for x and x' outside Σ, G^r must satisfy

$$\left[-\frac{\hbar^2 \nabla^2}{2m} + V(x) - E \right] G^r(x, x', E) = \hbar \delta(x - x') , \tag{2.20}$$

$$\langle x | G^r[\Sigma] G^r | x' \rangle = 0 . \tag{2.21}$$

Thus we find that we are allowed to use different G^r's which satisfy boundary conditions other than Dirichlet on Σ. (In appendix A we provide two simple examples in one dimension where eq. (2.17) is demonstrated with different restricted Green functions.)

2.3. THE MULTI-SURFACE DECOMPOSITION

The PDX expressions, eqs. (2.17), (2.18), can readily be extended to multiple decomposition surfaces. However, with multiple surfaces, the decomposition can be done in many ways, depending on what restricted Green functions we use, that is, depending on how we wish to regroup the paths. One way of doing this, which is particularly useful, is what we call the "sum over transitions", which is in effect a multiple scattering expansion of the full Green function.

Suppose we wish to break up $\mathcal{Q}$ into $p+1$ regions, such that there are p isolated "site" regions, labeled by an index $a = 1, 2, \ldots p$, each surrounded by a closed surface Σ_a (as shown in fig. 3 for the case $p = 3$). For instance each site might be a

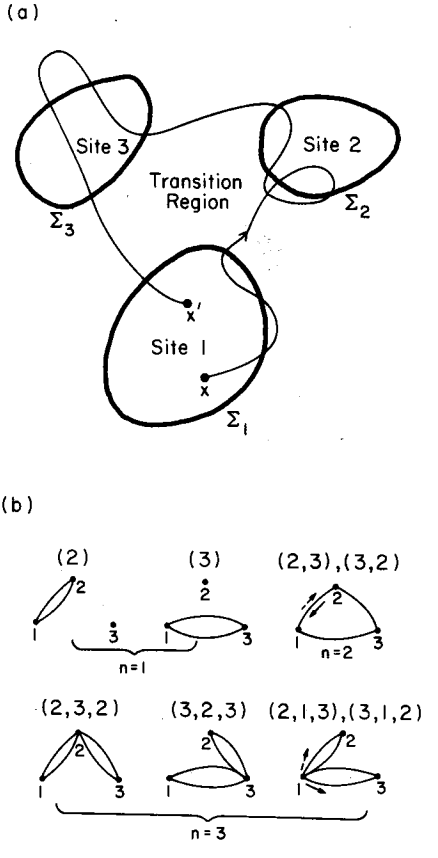

Fig. 3. The multiple surface decompositions $p = 3$. The terms of eq. (2.22) are labelled by integers $(a_1, a_2, \ldots, a_n)$ denoting the sequence of the sites that are visited. (a) A typical path contained in the term (2,3). The path is allowed to cross a surface Σ_i many times before making a transition to site $j \neq i$. (b) The different topology of the terms in eq. (2.22) is described by triple-vertex graphs. The vertices represent the sites, and the lines represent the transitions. All the terms up to 4 transitions ($n = 3$) are drawn.

well of a multiwell potential. We can then define a restricted Green function $G^{(a)}$ associated with each site. $G^{(a)}$ is defined to be the sum over all paths which never enter any site region *other* than a, and hence never cross any surface $\Sigma_{a'}$, $a' \neq a$. These functions will be called the "site" restricted Green functions. In addition, we define a restricted Green function over the "transition" region, G^{tr}, which is the sum over paths that never cross any of the surfaces. In the multiwell example G^{tr} is associated with the tunneling through the barrier. The sum over all paths in the full Green function can now be expressed as the sum over a multiple scattering series whose elements are labeled by an n-tuple of numbers specifying in sequential order the site regions that were visited. For instance, if x and x' are both in site 1,

$$G(x, x', E) = G^{(1)}(x, x', E) + \sum_{n=1}^{\infty} \sum_{a_1, a_2 \ldots a_n} \langle x | G^{(1)}[\Sigma_1] G^{\mathrm{tr}}[\Sigma_{a_1}] G^{(a_1)}[\Sigma_{a_1}]$$

$$\times G^{\mathrm{tr}}[\Sigma_{a_2}] G^{(a_2)} \ldots G^{(a_n)}[\Sigma_{a_n}] G^{\mathrm{tr}}[\Sigma_1] G^{(1)} | x' \rangle , \tag{2.22}$$

where $(n+1)$ specifies the number of transitions, and the n-tuples $(a_1, a_2, \ldots, a_n)$ specify the order in which sites are visited, hence the sum over a_j run from 1 to p subject to the restrictions $a_j \neq a_{j+1}$, $a_1 \neq 1$ and $a_n \neq 1$. Eq. (2.22) can be derived by expanding eq. (2.18) using eq. (2.17) iteratively. Each factor of $G^{(a)}$ represents the path segments that pass through region a and can cross its surface Σ_a many times, while G^{tr} represents the direct (no surface crossings) segments from one surface to another. Eq. (2.22) is therefore a path decomposition expansion of the full Green function into a sum of terms that contain *topologically distinct* classes of paths. We illustrate some of the first few terms of this series by their typical paths in fig. 3 for the triple-site ($p = 3$) case.

2.4. DIRECT SUM REPRESENTATION OF THE HAMILTONIAN

We begin this section by considering the double site problem $p = 2$. The results will be extended to the multiple site case at the end of this section. We first pick x_1 and x_1' to be both in region 1, and define the composite operator called the "bounce", $G^{\mathrm{b}}(E)$, which is the sum over all single return trips to region 2 (two transitions) which begin and end on Σ_1, but never enter region 1:

$$G^{\mathrm{b}} = [\Sigma_1] G^{\mathrm{tr}}[\Sigma_2] G^{(2)}[\Sigma_2] G^{\mathrm{tr}}[\Sigma_1] . \tag{2.23}$$

In fig. 4 a typical path in G^{b} is drawn. Now eq. (2.22) can be written as the geometric sum over bounces, which can be formally summed:

$$G(x_1, x_1', E) = \langle x_1 | G^{(1)} + G^{(1)} G^{\mathrm{b}} G^{(1)} + G^{(1)} G^{\mathrm{b}} G^{(1)} G^{\mathrm{b}} G^{(1)} + \cdots | x_1' \rangle$$

$$= \langle x_1 | \left[(G^{(1)})^{-1} - G^{(\mathrm{b})} \right]^{-1} | x_1' \rangle . \tag{2.24}$$

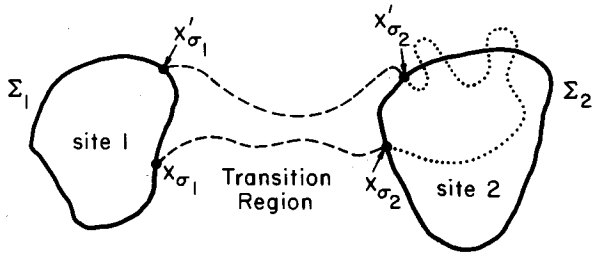

Fig. 4. The "bounce" in the 2-site problem. A typical path contained in the "bounce" Green function $G^{\mathrm{b}}(x_\sigma^1, x_\sigma^{1\prime}, E)$ of eq. (2.23) is drawn. The dashed segments contribute to the two factors of G^{tr}, and the dotted segments to the factor of $G^{(2)}$.

We can write the site restricted Green function $G^{(1)}$ as in eq. (2.19):

$$G^{(1)}(x, x', E) = -\hbar \sum_n \frac{\psi_n^{(1)*}(x)\psi_n^{(1)}(x')}{E - E_n^{(1)} + i\eta}. \tag{2.25}$$

In the following discussion we assume $G^{(1)}$ has a discrete real spectrum $E_n^{(1)}$, $n = 1, 2, \ldots$. The states $|\psi_n^{(1)}\rangle$ form a basis set in the restricted Hilbert space. The following operators can be represented as matrices:

$$G^{(1)}_{n,n'}(E) = \langle \psi_n^{(1)} | G^{(1)}(E) | \psi_{n'}^{(1)} \rangle = -\hbar [E - H^{(1)}]^{-1}_{n,n} \delta_{n,n'}, \tag{2.26}$$

$$H^{(1)}_{n,n'} = E_n^{(1)} \delta_{n,n'}, \tag{2.27}$$

$$G^{\mathrm{b}}_{n,n'}(E) = \langle \psi_n^{(1)} | G^{\mathrm{b}}(E) | \psi_{n'}^{(1)} \rangle. \tag{2.28}$$

Hence a matrix representation of G is obtained from

$$G(x_1, x_2, E) = -\hbar \sum_{n,n'} \psi_n^{(1)*}(x_1) \left[E - H^{(1)} + \hbar G^{\mathrm{b}}(E) \right]^{-1}_{n,n'} \psi_{n'}^{(1)}(x_1'). \tag{2.29}$$

From eq. (2.29) we can see that the poles, E_k, of the full Green function G, which have nonvanishing residues in region 1, obey the determinant condition

$$\det | E - H^{(1)} + \hbar G^{\mathrm{b}}(E) | |_{E = E_k} = 0. \tag{2.30}$$

Since eq. (2.30) does not assume $G^{(2)}$ has a discrete spectrum, we will be able to use it to calculate the decay rates of metastable states in sect. 3. For now, let us consider the case in which $G^{(2)}$ has only discrete poles. Thus when x and x' are not in region 1, $G^{(2)}(x, x', E)$ can be expressed analogously to $G^{(1)}$:

$$G^{(2)}(x, x', E) = -\hbar \sum_n \frac{\psi_n^{(2)*}(x)\psi_n^{(2)}(x')}{E - E_n^{(2)} + i\eta}. \tag{2.31}$$

It is convenient at this point to define an additional discrete representation using the states $|\psi_n^{(2)}\rangle$, such that

$$G^{(2)}_{n,n'}(E) = -\hbar[E - H^{(2)}]^{-1}_{n,n}\delta_{n,n'},$$

$$H^{(2)}_{n,n'} = E^{(2)}_n \delta_{n,n'}, \tag{2.32}$$

and define the transition matrix $M(E)$ which couples the two spaces:

$$M_{n,n'}(E) = \langle \psi_n^{(1)} | [\Sigma_1] G^{\mathrm{tr}} [\Sigma_2] | \psi_{n'}^{(2)} \rangle . \tag{2.33}$$

G^{b} can be written as the matrix product

$$G^{\mathrm{b}}(E) = M(E) G^{(2)}(E) M^{\dagger}(E). \tag{2.34}$$

So far, we have considered only the situation in which x and x' are both in region 1. It is straightforward to extend the analysis to the cases where one or both the endpoints lie outside of region 1. We can unify these expressions by constructing the direct sum representation, $|\psi_n^{(1)}\rangle \oplus |\psi_{n'}^{(2)}\rangle$. The result is an identity for $G(x, x', E)$ which holds for arbitrary x and x':

$$G(x, x', E) = -\hbar \sum_{ni;\, n'i'} \psi_n^{(i)*}(x)[E - \mathcal{H}(E)]^{-1}_{ni;\, n'i'} \psi_{n'}^{(i')}(x'), \tag{2.35}$$

where i, i' are the site indices, and $\psi_n^{(i)}(x)$ is the nth restricted eigenfunction which is defined to vanish inside the site j, $j \neq i$. $\mathcal{H}(E)$ is the "super-matrix" representation of the full hamiltonian

$$\mathcal{H}(E) = \begin{pmatrix} H^{(1)} & \hbar M(E) \\ \hbar M^{\dagger}(E) & H^{(2)} \end{pmatrix}. \tag{2.36}$$

The poles E_k of the full Green function obey the determinant condition

$$\det |E - \mathcal{H}(E)||_{E = E_k} = 0, \tag{2.37}$$

and the residues of eq. (2.35) at E_k, which are the eigenfunctions, are obtained as a linear combination of the restricted wave functions. Neither of the restricted basis sets $\psi_n^{(1)}$ nor $\psi_{n'}^{(2)}$ alone span the full Hilbert space, however their direct sum does. (Note: in cases of accidental degeneracies, when $M(E)$ has a pole at E_k, special care has to be taken in solving eq. (2.37), as in the example of appendix A.)

In eq. (2.35) the PDX provides us with a representation for the full hamiltonian of a system in terms of the restricted hamiltonians that have different boundary conditions in the different regions of space, and which are coupled by an energy-

dependent transition matrix $M(E)$. The direct sum space has an *overcomplete* basis of restricted wave functions, because their *support* overlaps in the transition regions between the sites. This accounts for the energy dependence of $\mathcal{H}(E)$ in this representation. In appendix A the 1D infinite square well example of the 2-site PDX is worked out and eq. (2.37) is used to find the poles of G.

We conclude this section by generalizing the treatment of the 2-site to the p-site problem ($p \geqslant 2$). The full hamiltonian can be written in a second-quantized notation as

$$\mathcal{H}(E) = H^{(1)} + H^{(2)} + \cdots + H^{(p)} + H^{\mathrm{tr}}(E),$$

$$H^{(i)} = \sum_n E_n^{(i)} a_{n,i}^\dagger a_{n,i}.$$

$$H^{\mathrm{tr}}(E) = \hbar \sum_{i,i'=1}^{p} \sum_{n,n'} \left[M_{n,n'}^{i,i'}(E) a_{n,i}^\dagger a_{n',i'} + \mathrm{h.c.} \right], \tag{2.38}$$

where $a_{n,i}^\dagger$ ($a_{n,i}$) is the creation (annihilation) operator of the restricted state $|\psi_n^{(i)}\rangle$, and M is the multiple site transition matrix

$$M_{n,n'}^{i,i'}(E) = \langle \psi_n^{(i)} | [\Sigma_i] G^{\mathrm{tr}} [\Sigma_{i'}] | \psi_{n'}^{(i')} \rangle. \tag{2.39}$$

The full Green function $G(x, x', E)$ can be constructed in terms of restricted states in a fashion analogous to eq. (2.34):

$$G(x, x', E) = -\hbar \sum_{i,i'=1}^{p} \sum_{n,n'} \psi_n^{(i)*}(x) \psi_{n'}^{(i')}(x') \langle \psi_n^{(i)} | \frac{1}{E - \mathcal{H}(E)} | \psi_{n'}^{(i')} \rangle. \tag{2.40}$$

3. Multidimensional tunneling

3.1. INTRODUCTION

Tunneling is a phenomenon which involves the leakage of a wave function through a classically forbidden ("barrier") region of the potential separating two or more classically allowed ("well") regions. The notion of the forbidden and allowed regions is dependent on the energy E of the system. Thus we are led in this part of the paper to study the energy Green function, $G(x, x', E)$, at energies which are (much) less than the barrier heights.

Tunneling is one of the most obviously non-classical manifestations of quantum mechanics; there is an entirely non-classical energy scale which is dynamically generated by it. To be more explicit, let us consider a simple problem of the sort

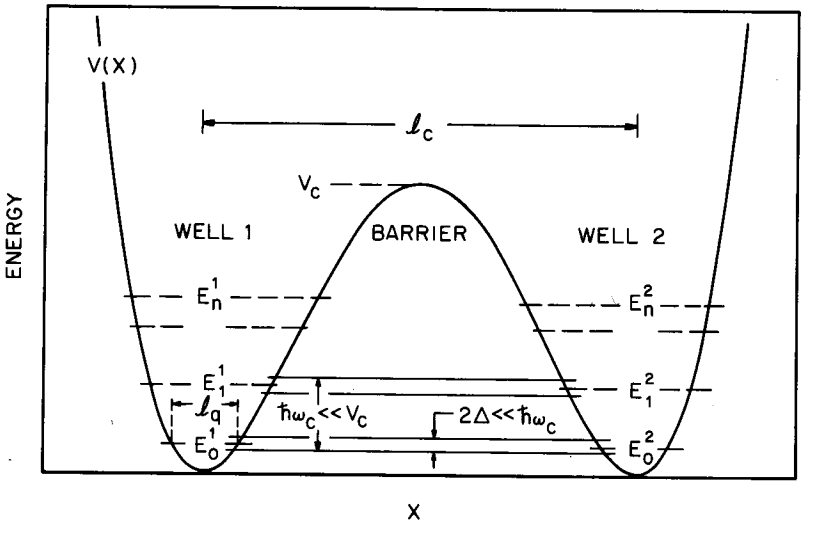

Fig. 5. Characteristic scales in a generic symmetric double well problem. The low-lying poles of the two "well" Green functions are marked as dashed lines. The solid lines represent the poles of the full Green function. $V(x)$ is the potential projected on the x-coordinate, l_c, l_q, ω_c, and Δ are defined in the text (eqs. (3.1), (3.2)).

shown in fig. 5 in which the potential energy can be characterized by a single magnitude V_c, say the barrier height, and a single spatial length scale l_c, which might be the separation between wells. In addition to these, there is one more independent dimensional quantity which characterizes the classical dynamics, a frequency ω_c which can be a characteristic small oscillation frequency in the inverted barrier, i.e.

$$\omega_c \sim \sqrt{\frac{V_c}{ml_c^2}} \,. \tag{3.1}$$

In the corresponding quantum problem, non-tunneling phenomena can be characterized by two energy scales, V_c and $\hbar\omega_c$, which are simply related to the classical motion. However tunneling produces effects with energies of order

$$\Delta = A\hbar\omega_c \exp\left[-B(V_c/\hbar\omega_c)\right], \tag{3.2}$$

where A and B are numbers of order 1. In the interesting regime of parameter space, where the barrier height is large compared to the quantum zero-point energy, $V_c \gg \hbar\omega_c$, Δ is much smaller than the other characteristic energies and any approximation used in solving the non-tunneling part of the problem will almost certainly result in errors that are large compared to Δ. Thus we must employ a non-perturbative technique to solve the problem, and we must think carefully to

determine which of the results we obtain are meaningful despite the presence of other errors that are large compared to Δ. (Note: the fact that Δ is so small compared to all other energy scales presents difficulties in the direct numerical integration of the Schrödinger equation.)

To focus our thinking we start by rescaling the potential, energy, coordinates, and time to express the path integral in terms of convenient dimensionless variables:

$$\begin{aligned} V(x)/V_c &\mapsto V(x), \\ E/V_c &\mapsto E, \\ x/l_c &\mapsto x, \\ \omega_c t &\mapsto t, \end{aligned} \tag{3.3}$$

and hence the action will be rescaled as

$$S[x]/\hbar = (1/\hbar)\int_0^T \mathrm{d}t\left[\tfrac{1}{2}m\dot{x}^2 - V(x)\right] \mapsto (1/g)\int_0^T \mathrm{d}t\left[\tfrac{1}{2}\dot{x}^2 - V(x)\right], \tag{3.4}$$

where g is the dimensionless quantum parameter given by

$$g = \hbar\omega_c/V_c = \left(l_q/l_c\right)^2, \tag{3.5}$$

and l_q is the quantum length scale $\sqrt{\hbar/m\omega_c}$. g is a dimensionless measure of the importance of $\hbar$. In the simple case where the classical potential has only one characteristic magnitude and length scale, they are all of order 1. All small amplitude oscillation frequencies are also of order 1. (The case in which there are many very different frequency scales in the classical problem is treated explicitly in subsect. 3.4 and in sect. 4.)

Our approach to the tunneling problem, which can be called a semiclassical or small-$\hbar$ approximation, is to obtain an asymptotic expansion for $G(x_1, x_2, E)$ for small $g \ll 1$. This implies the well-known result that the path integral

$$G(x_1, x_2, E) = i\int_0^\infty \mathrm{d}t \int_{x_1}^{x_2} \mathcal{D}[x]\exp\left[\frac{i}{g}\left(S[x] + Et\right)\right] \tag{3.6}$$

can be evaluated by the method of steepest descents, which in turn implies that it is dominated by paths in the neighborhood of the classical path with energy E (the saddle points). There are three difficulties with this approach:

(i) There are, by definition, no classical paths in the classically forbidden region. This difficulty is easily surmounted since by "classical" paths we merely mean paths which satisfy the Euler-Lagrange equations $\delta S = 0$ and $\partial S/\partial t = E$. Thus, we search

for solutions evolving in imaginary time, or *equivalently* for solutions of the real equations of motion with energy $-E$ in the inverted potential $-V(x)$.

(ii) The classical paths in the classically allowed region are very complicated. There are an infinite number of them, and generally they are chaotic. Note, however, that the classical paths in the forbidden region are very simple since in the inverted potential any path which wanders too far in any direction typically falls off to infinity. Moreover, since in the forbidden region the argument of the exponent in eq. (3.6) is real and negative, any long meandering classical paths which do occur make almost no contribution to the path integral since they will have a very large action.

(iii) There is no obvious way to connect the classical path contributions in the allowed and forbidden regions, in more than one dimension.

Problems (ii) and (iii) can be neatly avoided using the PDX. We define a decomposition surface that encloses each well. The restricted Green function G^{well} associated with a well can typically be computed in some other way. *It does not involve tunneling*, and so there is no reason to treat it in the same way as we treat a tunneling problem. Often, at low energies a well is approximately harmonic and hence G^{well} can be computed quite accurately by perturbation theory. (In the model problems solved in sect. 4 this will be the case.) Alternatively, the well might be associated with an atom, and G^{well} could be computed using some version of the quantum defect method. If nothing else avails, one could compute it by direct numerical integration of the Schrödinger equation. The important point is that G^{well} does not have to be computed using classical paths and so problem (ii) is finessed. The PDX itself is a connection formula, and is the solution to problem (iii). One technical point that is worth mentioning at the outset concerns the choice of decomposition surface. Since we wish to include only imaginary-time paths in the restricted Green function of the barrier region, the surfaces should lie in the classically forbidden region. An obvious choice of the surfaces are the surfaces of energy E, $V(x) = E$, which separate the allowed from forbidden regions. This turns out *not* to be a convenient choice since the semiclassical approximation breaks down when the endpoints lie on such a surface as reflected in the divergence of the prefactor [5] (which is proportional to the square root of the inverse classical velocity at the endpoint). However, since by assumption $l_q \ll l_c$, we can choose the decomposition surface Σ to be many quantum length scales l_q outside the allowed region, while still having a good approximation for G^{well} evaluated at Σ.

We shall show that the surface integration, too, can usually be performed by steepest descents. As a result, the entire tunneling process is dominated by paths in the vicinity of a single classical path of energy $-E$ (the "instanton path"), which originates and terminates at uniquely determined points on the two decomposition surfaces of the neighbouring wells. (We call them the "instanton points".)

In subsect. 3.2 the direct-sum representation of the hamiltonian of eq. (2.36) is truncated so that we can better study the low-lying states of two wells coupled by the tunneling matrix elements. In subsect. 3.3 we show explicitly how to compute a PDX

expression in the semiclassical approximation. Specifically the wave functions in the forbidden region and the tunneling matrix elements of the truncated hamiltonian are computed. In subsect. 3.4 we discuss the separation of time scales, which enables us to simplify a given problem by reducing a many-dimensional tunneling calculation to one involving fewer, important degrees of freedom. Subsect. 3.5 is a summary and outline of the strategy for solving a multidimensional tunneling problem in a real physical system which has been developed in this part of the paper.

3.2. THE TRUNCATED HAMILTONIAN OF THE MULTIDIMENSIONAL DOUBLE WELL

In this section we consider only the double well problem although, as with the two-site PDX which was discussed in subsect. 2.3, its generalization to multiple wells is straightforward. We wish to calculate the properties of the system at energies small compared to the height of the barriers between wells. (In the rescaled units of subsect. 3.1 this means $E \ll 1$.) We define two decomposition surfaces Σ_1 and Σ_2 which each enclose one well, thus breaking configuration space into three disjoint regions. Three restricted Green functions are thus defined: $G^{(1)}$ restricted outside well 2, $G^{(2)}$ outside well 1, and G^{tr} outside both wells. We first consider the case in which the spectrum in both wells is discrete, so we can use eq. (2.38) to obtain the representation of the full hamiltonian in the direct sum space of the restricted eigenstates of the two wells:

$$\mathcal{H}(E) = \sum_n E_n^{(1)} a_n^\dagger a_n + \sum_{n'} E_{n'}^{(2)} b_{n'}^\dagger b_{n'} + \sum_{n,n'} \left[M_{n,n'}(E) a_n^\dagger b_{n'} + \text{h.c.} \right], \tag{3.7}$$

where a_n ($b_{n'}$) is the annihilation operator of state $\psi_n^{(1)}$ ($\psi_{n'}^{(2)}$), and

$$M_{n,n'}(E) = \langle \psi_n^{(1)} | [\Sigma_1] G^{\mathrm{tr}}(E) [\Sigma_2] | \psi_{n'}^{(2)} \rangle \tag{3.8}$$

is the tunneling matrix which couples the two wells. If the wells have quadratic minima, for example, one would use harmonic oscillator wave functions as the states of the wells, and improve on them by perturbation theory in the anharmonic terms of the potential. Thus we can generally find the low-lying energies $E_n^{(i)}$ and wave functions at the surface $\psi_n^{(i)}(\boldsymbol{x}_{\sigma_i})$ $i = 1, 2$ up to errors of order g^ν, $\nu \geqslant 2$. In the following subsection, subsect. 3.3, $M_{n,n'}$ will be explicitly evaluated and shown to be of order

$$M_{n,n'}(E) \sim g\, \mathrm{e}^{-W(E)/g} \ll g^\nu \ll 1, \qquad \nu \geqslant 2, \tag{3.9}$$

since $W(E) \sim 1$ at low energies. Let us examine the low-lying spectrum of $\mathcal{H}(E)$. The level spacings in each well (for the non-continuum case) is of order $\hbar\omega_c = g$. Any coupling between two states which have energy difference larger or of order g will produce a negligibly small shift in their energies since by perturbation theory in M the shifts are of order $g\, \mathrm{e}^{-2W(E)/g}$ and thus smaller than the initial errors in the

restricted states. Thus we can usually ignore all the tunneling matrix elements which connect two such states and leave only the tunneling matrix elements that connect near degenerate states $|E_n - E_{n'}| \ll \hbar\omega_c = g$. The E-dependence of M can thus be eliminated by replacing all the important elements by E-independent averages:

$$\overline{M}_{n,n'} = \begin{cases} M_{n,n'}\left(\frac{1}{2}(E_n + E_{n'})\right), & |E_n - E_{n'}| \ll g \\ 0 & \text{otherwise.} \end{cases} \tag{3.10}$$

Negligible errors are introduced by this substitution as can be seen from the fact that $\partial \log M(E)/\partial E \sim g^{-1}$. Thus we end up with a truncated E-independent hamiltonian $\overline{\mathcal{H}}$ which includes only the low-lying states of the two independent wells, and some relevant tunneling matrix elements (which we shall learn to compute in the next section).

$\overline{\mathcal{H}}$ reproduces the semiclassically calculable tunneling effects in the system, such as the splitting of degenerate energy levels and the admixture of restricted states. However we point out that there are tunneling effects which cannot be calculated within a consistent semiclassical approach, which include the amplitude leakage of the wave function between restricted states which are *uncoupled* in $\overline{\mathcal{H}}$. This is closely related to the known difficulty in the one-dimension WKB approximation when applied to the asymmetric double well problem*. The source of that difficulty lies in the necessary admixture of the exponentially growing solution with the exponentially decaying one when connecting the wave function of the allowed region to the forbidden region. This admixture cannot be calculated consistently to high enough accuracy.

In the case where there is a continuum of states in region 2, $G^{(2)}$ is not pure real and its imaginary part is proportional to $F^{(2)}$:

$$\mathrm{Im}\, G^{(2)}(x, x', E) = -g\pi F^{(2)}(x, x', E), \tag{3.11}$$

which has as diagonal elements the local density of states

$$F^{(2)}(x, x, E) = \sum_n \left|\psi_n^{(2)}(x)\right|^2 \delta\left(E - E_n^{(2)}\right). \tag{3.12}$$

In this case the poles E_n of G should be evaluated directly from the sum over bounces, i.e. the determinant equation eq. (2.30). It is clear that tunneling results in an unimportant, exponentially small shift of the pole $E_n^{(1)}$ proportional to $\mathrm{Re}\, G^{(2)}$ and a similarly small imaginary shift which is the leading-order contribution to the imaginary part of E_n and can be interpreted as the decay rate of a metastable state

$$E_n = E_n^{(1)} + \tfrac{1}{2} i\Gamma_n, \tag{3.13}$$

* We thank Dr. Martin Gutzwiller for pointing out to us this difficulty in the WKB method.

where

$$\tfrac{1}{2}\Gamma_n = g\,\mathrm{Im}G^{\mathrm{b}}_{n,n}\big(E_n^{(1)}\big) = -g^2\pi\langle\psi_n^{(1)}|[\Sigma_1]G^{\mathrm{tr}}[\Sigma_2]F^{(2)}[\Sigma_2]G^{\mathrm{tr}}[\Sigma_1]|\psi_n^{(1)}\rangle\,. \tag{3.14}$$

In the cases where $F^{(2)}$ can be factorized (as in one dimension),

$$F^{(2)}(x, x', E) = \psi_E^{(2)}(x)\psi_E^{(2)}(x')\rho(E)\,. \tag{3.15}$$

Γ_n is expressed by a simpler version of eq. (3.14):

$$\tfrac{1}{2}\Gamma_n = -g^2\pi\left|\langle\psi_n^{(1)}|[\Sigma_1]G^{\mathrm{tr}}\big(E_n^{(1)}\big)[\Sigma_2]|\psi_{E_n}^{(2)}\rangle\right|^2\rho(E)\,, \tag{3.16}$$

which is the familiar "Fermi golden rule" as it applies to the tunneling decay process.

Again the spectrum can be represented by a truncated hamiltonian $\overline{\mathcal{H}}$. In this case, however, $\overline{\mathcal{H}}$ is purely diagonal and has complex matrix elements E_n; it is thus non-hermitian.

3.3. PDX AND THE SEMICLASSICAL APPROXIMATION

This subsection is technical in nature. It provides the steps needed in order to calculate a PDX expression in the semiclassical approximation. The main task of this subsection is to arrive at a calculable formula for the tunneling matrix element $M_{n,n'}(E)$ introduced in eq. (3.8) such that the tunneling effects in the truncated system described in the previous subsection section (3.2) can be computed.

For pedagogical reasons we begin by evaluating the single well wave function ψ_n of energy E_n at position y, where y is deep in the forbidden region, i.e. $V(y) \gg E_n$. $\psi_n(y)$ is obtained using the semiclassical approximation to the single surface PDX expression, eq. (2.17). We pick the decomposition surface Σ to lie in the forbidden region, and take the residue of both sides of eq. (2.17) at $E = E_n$. This leads to the equation

$$\psi_n(y) = \int_\Sigma \mathrm{d}x_\sigma \psi_n(x_\sigma)C(x_\sigma, y, E_n)\,, \tag{3.17a}$$

where

$$C(x_\sigma, y, E) = -\tfrac{1}{2}g(\hat{n}\cdot\nabla)G^{\mathrm{r}}(x, y, E)_{x=x_\sigma}\,. \tag{3.17b}$$

C can be evaluated using the semiclassical approximation to the restricted Green function G^{r}. (The reader is referred to ref. [5] for a comprehensive review of the semiclassical energy Green function, and to ref. [6] for the treatment of hard walls). The result is

$$C(x_\sigma, y, E) = A(x_\sigma, y, E)\exp\left[-\frac{1}{g}W(x_\sigma, y, E)\right][1 + \mathrm{O}(g)]\,, \tag{3.18}$$

where the quantities on the right-hand side depend on the dynamics of the classical path $x_c(t)$ which is the solution to the equations

$$\ddot{x}_c(t) - \nabla V(x_c(t)) = 0, \tag{3.19a}$$

$$\tfrac{1}{2}\dot{x}_c^2(t) - V(x_c(t)) = -E, \tag{3.19b}$$

subject to the boundary conditions

$$x_c(0) = x_\sigma, \qquad x_c(T) = y, \tag{3.19c}$$

with $T = T(x_\sigma, y, E)$. Thus $x_c(t)$ is the classical path with energy $-E$ which obeys Newton's equations of motion in the *inverted* potential. In principle more than a single path can obey eqs. (3.19). However, by imposing general restrictions on the behavior of the potential, we shall discard this additional complication. Having found $x_c(t)$ we can express the action W, the time T, and the prefactor A as

$$W(x_\sigma, y, E) = \int_{x_\sigma}^{y} \mathrm{d}x_c \sqrt{2(V(x_c) - E)}\,, \tag{3.20}$$

$$T(x_\sigma, y, E) = \frac{\partial W}{\partial E}(x_\sigma, y, E), \tag{3.21}$$

$$A(x_\sigma, y, E) = \hat{n} \cdot v(0) \left[\frac{\Delta_1}{v(0)v(T)} \right]^{1/2}, \tag{3.22a}$$

$$\Delta_1 = \det' \left| \hat{\eta}_i(0) \cdot \frac{\partial^2 W}{\partial x\, \partial y} \cdot \hat{\eta}_j(T) \right| \left(\frac{-1}{2\pi g} \right)^{N-1}, \tag{3.22b}$$

where $v \equiv \dot{x}_c$. The unit vectors $\hat{\eta}_i(t)$, $i = 1, N$ are an orthonormal basis set chosen such that $\hat{\eta}_1(t)$ is parallel to $v(t)$ for $t = 0, T$. The matrix in the determinant of eq. (3.22b) has indices i, j; $i, j = 2, N$. The prime denotes projecting out the $i = 1$ and $j = 1$ components.

In many non-separable cases the surface integration of eq. (3.17a) can be performed by steepest descents. This is possible whenever the integrand in eq. (3.17a) is highly peaked in the vicinity of an "instanton point" $\bar{x}_\sigma \in \Sigma$. The prefactor $A(x_\sigma, y, E)$ in eq. (3.18) is a slowly varying function of x_σ, so $C(x_\sigma, y, E)$ is peaked at the point $\bar{x}_\sigma$ where $W(x_\sigma, y, E)$ is minimal. Since the gradient of the action with respect to its initial point is the negative of the initial momentum of the classical path, the condition that W be minimal is equivalent to the condition that the classical trajectory from $\bar{x}_\sigma$ to y must leave the surface perpendicularly. In general there are potentials and surfaces where this condition can be satisfied by many

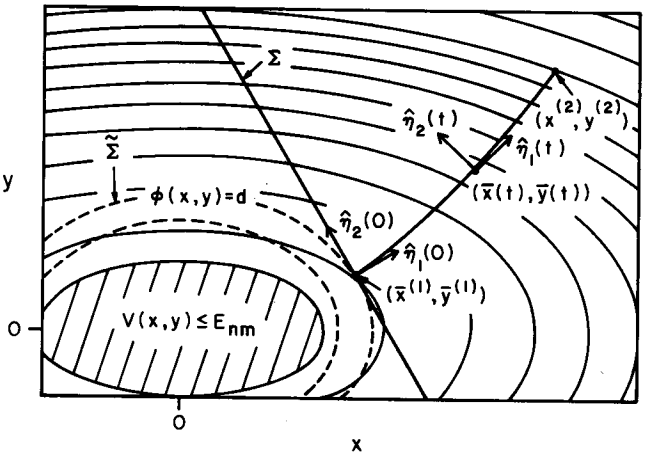

Fig. 6. The semiclassical calculation of the 2-dimensional harmonic oscillator wave function $\psi_{nm}(x^{(2)}, y^{(2)})$ which is carried out in appendix C. The solid contours are equipotential curves, and the dashed contours are the surfaces of constant wave function (ϕ). The shaded area is the allowed region $E_{nm} \geq V$, and Σ is the decomposition surface which is perpendicular to the instanton path of zero energy $\bar{x}$, $\bar{y}$, and tangent to the surface of constant wave function $\tilde{\Sigma}$. $\hat{\eta}_1(t)$ and $\hat{\eta}_2(t)$ are the parallel transported basis vectors of the fluctuations defined in eqs. (3.26).

instanton points, but, for the sake of simplicity in the following discussion, let us restrict ourselves to study the cases where only a single instanton point exists. In order to simplify the steepest descents evaluation of the surface integral in eq. (3.17a) we use our freedom in picking the decomposition surface to choose Σ in such a way that $\psi_n(\boldsymbol{x}_\sigma)$ is maximal at $\bar{\boldsymbol{x}}_\sigma$ as well. We can construct such a surface in the following manner: first we consider a surface $\tilde{\Sigma}$ of constant wave function, well inside the forbidden region. (Fig. 6 illustrates this procedure for the 2D harmonic oscillator wave functions which are computed semiclassically in appendix C). We find the instanton point on this surface according to the above prescription. We then choose the decomposition surface Σ to be locally flat and tangent to $\tilde{\Sigma}$ at the point $\bar{\boldsymbol{x}}_\sigma$. (Since the only important contributions to the steepest descents evaluation of the integral come from the region of radius $\sim l_q \sim \sqrt{g}$ about $\bar{\boldsymbol{x}}_\sigma$, Σ need be flat only over a distance large compared to l_q.) Now, by construction, $\bar{\boldsymbol{x}}_\sigma$ is an extremal point of ψ. Since we are interested in cases in which ψ decays with distance from the well, we expect $\tilde{\Sigma}$ to curve "inwards" as shown in fig. 6, and hence the wave function is also maximal at the instanton point.

We express $\psi_n(\boldsymbol{x}_\sigma)$ as

$$\psi_n(\boldsymbol{x}_\sigma) = p(\boldsymbol{x}_\sigma)\exp\left[-\frac{1}{g}\phi(\boldsymbol{x}_\sigma)\right]. \tag{3.23}$$

In some cases the wave function is *not* well behaved at the instanton point. In this

case the surface integration cannot be performed by steepest descents but, rather must be carried out more carefully. For example, if the potential is separable, i.e. $V=\Sigma_i^N V(x_i)$, and if we are interested in a perpendicularly excited state n, $p(x_\sigma, n)$ may oscillate rapidly in the vicinity of the instanton point. However, separable potentials need not be handled by the multidimensional PDX. In some other situations, where a perpendicular coordinate is an adiabatic "slave" along the instanton path, one can use the adiabatic fluctuations approximation (AFA) which is discussed in appendix D. In the following discussion we shall assume that in eq. (3.23) p and ϕ (which depend on n) are slowly varying functions of x_σ in the vicinity of the instanton point.

Thus, the integrand of eq. (3.17a), I_n in the vicinity of $\bar{x}_\sigma$ can be expanded in powers of $(x_\sigma - \bar{x}_\sigma)$:

$$I_n = p(\bar{x}_\sigma) A(\bar{x}_\sigma, y, E) \exp\left\{ -\frac{1}{g}\left[\phi(\bar{x}_\sigma) + W(\bar{x}_\sigma, y, E_n) + \tfrac{1}{2} \sum_{j,j'=2}^{N} x_j x_{j'} \left(W_{jj'}^{11} + \phi_{jj'} \right) \right] \right\} \left[1 + \sum_j \mathrm{O}(x_j) \right], \tag{3.24a}$$

where

$$x_j = (x_\sigma - \bar{x}_\sigma) \cdot \hat{\eta}_j(0), \tag{3.24b}$$

and we denote

$$W_{ij}^{\alpha\beta} \equiv \frac{\partial^2}{\partial x_i^{(\alpha)} \partial x_j^{(\beta)}} W(x^{(1)}, x^{(2)}, E), \qquad \alpha, \beta = 1, 2. \tag{3.24c}$$

We can use the same basis vectors $\hat{\eta}_j(0)$, $j=2, N$ as in eq. (3.22b), since by construction Σ is normal to $\hat{\eta}_1(0)$. The steepest descent integration of eq. (3.24a) over Σ can now be performed to yield

$$\psi_n(y) = \Lambda_n(\bar{x}_\sigma, y, E_n) \psi_n(\bar{x}_\sigma) \exp\left[-\frac{1}{g} W(\bar{x}_\sigma, y, E_n) \right] [1 + \mathrm{O}(g)], \tag{3.25a}$$

where

$$\Lambda_n(\bar{x}_\sigma, y, E_n) = \left| \frac{v(0)}{v(T)} \frac{\Delta_1}{\Delta_2} \right|^{1/2}, \tag{3.25b}$$

where v is the magnitude of $\bar{v}$, Δ_1 is defined in eq. (3.22b), and

$$\Delta_2 = \det'|W_{ij}^{11} + \phi_{ij}| \left(\frac{1}{2\pi g} \right)^{N-1} . \tag{3.25c}$$

The prefactor Λ_n is the measure of the contribution of paths in the vicinity of the instanton path. It can also be computed in terms of solutions to the linearized *classical* equations of motion for the fluctuations around the instanton path, also called the "variational equations of Jacobi or Poincaré" [7]. The fluctuations are denoted by the vector functions $\boldsymbol{q}^j(t)$, $t \in [0, T]$, which obey

$$\ddot{\boldsymbol{q}}^j = \frac{\partial^2 V(\bar{x})}{\partial x \, \partial x'} \cdot \boldsymbol{q}^j , \qquad j = 2, N,$$

where the index j denotes that $q^j(t)$ satisfies the initial condition $\boldsymbol{q}^j(0)$ is parallel to $\hat{\eta}_j(0)$. These equations yield $N-1$ stability frequencies which can be incorporated into the instanton action as a potential renormalization (see subsect. 4.5 for a model problem in which this effect can be dramatic). This alternate description of the prefactor is derived in detail in appendix B, much in the same way as Gutzwiller derived the stability angles for the semiclassical energy levels [8] (the analysis of Gutzwiller was extended to field theories by Dashen et al.). The main differences between this and the energy levels analysis is that here we are looking at a classical path in imaginary time (forbidden region) with positive stability angles (definite instability) between *different* endpoints, and in the other case the complex stability angles are calculated for a *periodic* orbit in the allowed region. We briefly present the results of appendix B. It is convenient to express the fluctuations equations in terms of the *parallel-transported* moving frame $\{\hat{\eta}_i(t)\}$, which coincides with the frames $\{\hat{\eta}_i(0)\}$ and $\{\hat{\eta}_i(T)\}$ at $t = 0$ and $t = T$ respectively. The parallel transport is defined by

$$\hat{\eta}_1(t) = \frac{\bar{v}(t)}{v(t)} , \tag{3.26a}$$

$$\hat{\eta}_i(t) \cdot \hat{\eta}_j(t) = 0 , \quad i, j = 1, N, \tag{3.26b}$$

$$\dot{\hat{\eta}}_i(t) \cdot \hat{\eta}_j(t) = 0 , \quad i, j = 2, N. \tag{3.26c}$$

This enables us to reduce the N coupled equations for the fluctuations to $N-1$ equations for the projection of the fluctuations onto a hyperplane perpendicular to the instanton path. Thus, $q_{ij} \equiv \hat{\eta}_i \cdot \boldsymbol{q}^j$ obey the equations

$$\ddot{q}_{ij}(t) = \sum_{i'=2, N} \left[\Omega_{ii'}^2(t) - 3\delta_{ii'} J_{1i'}^2(t) \right] q_{i'j}(t) , \qquad i, j = 2, N, \tag{3.27a}$$

with the initial conditions

$$q_{ij}(0) = \delta_{ij}, \qquad \dot{q}_{ij}(0) = \phi_{ij}. \tag{3.27b}$$

Here, the "transverse curvatures" are

$$\Omega_{ij}^2(t) = \hat{\eta}_i(t) \cdot \frac{\partial V(\bar{x}(t))}{\partial x \, \partial x'} \cdot \hat{\eta}_j(t) \tag{3.27c}$$

and the "bending frequencies" are

$$J_{1j}(t) = \dot{\hat{\eta}}_1(t) \cdot \hat{\eta}_j(t) \tag{3.27d}$$

for $i, j = 2, N$. In terms of the solutions of this equation, Λ_n is given by the expression

$$\Lambda_n = \left[\frac{v(0)}{v(T)}\right]^{1/2} \det'|q_{ij}(T)|^{-1/2} = \left[\frac{v(0)}{v(T)}\right]^{1/2} \exp\left[-\tfrac{1}{2} \sum_{k=2,N} \nu_k T\right], \tag{3.28}$$

where again det′ is an $(N-1)^2$-dimensional determinant $(i, j = 2, N)$, and the $(N-1)$ stability frequencies $\nu_k(T)$ correspond to the eigenvalues of q_{ij}.

In appendix C the two-dimensional harmonic oscillator wave functions are worked out to provide an explicit example. An exact calculation of the instanton path and fluctuations is demonstrated. In other potentials the analytic solutions for the *classical* dynamics are not available in closed form, and one has to resort to numerical methods or approximations.

We proceed to the more complicated problem of calculating the tunneling matrix element $M_{n,n'}(E)$ of eq. (3.8). This involves two surface integrations: on Σ_1 and Σ_2. The two restricted wave functions $\psi_n^{(1)}$ and $\psi_{n'}^{(2)}$ are written as in eq. (3.23) thus defining the exponential functions $\phi^{(1)}(x_\sigma^{(1)})$ and $\phi^{(2)}(x_\sigma^{(2)})$ respectively. (The indices n and n' will sometimes be dropped to avoid cluttering the notation.) We choose the surfaces of constant wave functions $\tilde{\Sigma}_i$, $i = 1, 2$ in the forbidden region, and find the instanton path $\bar{x}(t)$ of energy $-E$ in the inverted potential such that its initial and final velocities are perpendicular to Σ_1 and Σ_2 respectively. Again, we choose Σ_i to be the tangent surface to $\tilde{\Sigma}_i$ at $\bar{x}_\sigma^i$. In fig. 7 these surfaces and the instanton path are illustrated. As in the previous case, we use the steepest descent integration simultaneously on both surfaces to arrive at

$$M_{n,n'}(E) = \Lambda_{n,n'} \psi_n^{(1)}(\bar{x}_\sigma^{(1)}) \psi_{n'}^{2*}(\bar{x}_\sigma^{(2)}) \exp\left[-\frac{1}{g} W(\bar{x}_\sigma^{(1)}, \bar{x}_\sigma^{(2)}, E)\right][1 + O(g)], \tag{3.29a}$$

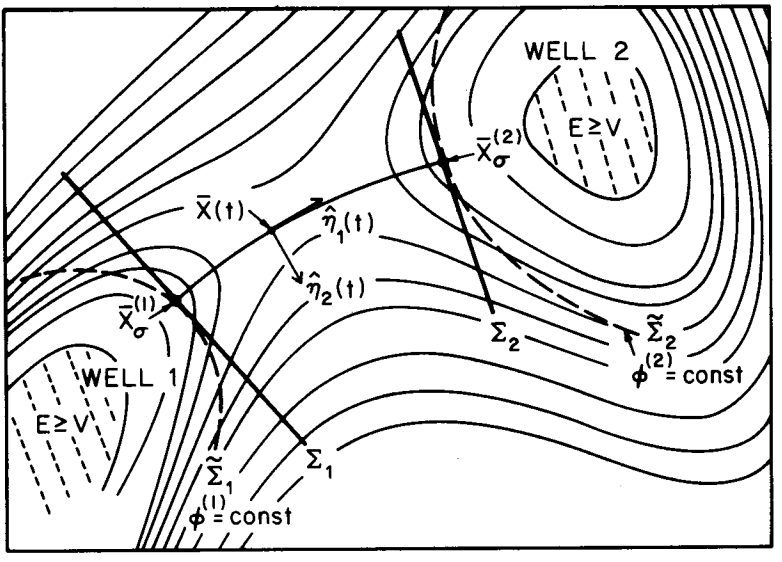

Fig. 7. The semiclassical calculation of the tunneling matrix element $M(E)$. The solid contours are equipotential curves, and the dashed contours are the surfaces of constant restricted wave functions. The shaded areas are the allowed regions $E \geq V$, and Σ_i, $i = 1,2$ are the decomposition surfaces which are perpendicular to the instanton path $\bar{x}$ of energy $-E$. $\hat{\eta}_1(t)$ and $\hat{\eta}_2(t)$ are the parallel transported basis vectors of the fluctuations defined in eq. (3.26).

where

$$W\left(\bar{x}_\sigma^{(1)}, \bar{x}_\sigma^{(2)}, E\right) = \int_{\bar{x}_\sigma^{(1)}}^{\bar{x}_\sigma^{(2)}} \mathrm{d}\bar{x} \sqrt{2[V(\bar{x}) - E]}\,, \tag{3.29b}$$

$$\Lambda_{n,n'} = [v(0)v(T)]^{1/2} \left[\frac{\Delta_1}{\Delta_3}\right]^{1/2},$$

$$\Delta_1 = \left(-\frac{1}{2\pi g}\right)^{N-1} \det' |W_{ij}^{12}|,$$

$$\Delta_3 = \left(-\frac{1}{2\pi g}\right)^{2(N-1)} \det' \begin{vmatrix} W_{ij}^{11} + \phi_{ij}^{(1)} & W_{ij}^{12} \\ W_{ij}^{21} & W_{ij}^{22} + \phi_{ij}^{(2)} \end{vmatrix}. \tag{3.29c}$$

(The superscripts α, β in $W_{ij}^{\alpha\beta}$ denote the arguments to which the derivatives ∂_i, ∂_j are applied respectively.) The prefactor $\Lambda_{n,n'}$ can be expressed in terms of the same fluctuations q_{ij} which are the solutions of eqs. (3.27) but where in the initial

conditions eqs. (3.27b) $\phi_{ij}^{(1)}$ is substituted for ϕ_{ij}. The result is

$$\Lambda_{n,n'} = \det'|\dot{q}_{ij}(T) + J_{1i}(T)q_{1j}(T) + \sum_{i'=2,N} \phi_{ii'}^{(2)} q_{i'j}(T)|^{-1/2}$$

$$\times (2\pi g)^{(N-1)/2}[v(0)v(T)]^{1/2}, \tag{3.30a}$$

where the "longitudinal" fluctuation, $q_{1j}(T)$, which appears here, can be expressed in terms of the transverse fluctuations according to

$$q_{1j}(T) = 2v(T) \sum_{i=2,N} \int_0^T \mathrm{d}t \, \frac{J_{1i}(t)q_{ij}(t)}{v(t)} . \tag{3.30b}$$

Again, this prefactor can also be expressed in terms of the stability frequencies, as in eq. (3.28), and the dimensional quantum lengths l_k which cancel the $N-1$ length dimensions of the wave functions normalization,

$$\Lambda_{n,n'} = [v(0)v(T)]^{1/2} \left(\prod_{k=2}^{N} l_k \right) \exp\left[-\tfrac{1}{2} \sum_{k=2,N} \nu_k T \right], \tag{3.31a}$$

where

$$l_k = \sqrt{g\pi/\nu_k} . \tag{3.31b}$$

While the solution of the fluctuation equations is often complicated, good approximated solutions can often be obtained. In appendix D the adiabatic fluctuations approximation is presented. It is the adiabatic approximation for the dynamics of the transverse coordinates, and can be valid even when the naive semiclassical approximation for G^{tr} and the steepest-descent integration of the surfaces is not, as shown by an explicit example in subsect. 4.5. The approximation is valid when the curvatures (3.27c) and bending frequencies (3.27d) are slowly varying along the instanton path. In this case,

$$\nu_k(T)T \simeq \int_0^T \mathrm{d}t \, \Omega_k(\bar{x}(t)), \tag{3.32a}$$

where Ω_k are the eigenvalues of Ω_{ij} of eq. (3.27c). Using eq. (3.32a) we can replace $\Lambda_{n,n'}$ with a *local* renormalization of the potential, such that $V(\bar{x})$ is replaced by $V^{\mathrm{ren}}(\bar{x})$ in the instanton action W, where

$$V^{\mathrm{ren}}(\bar{x}) = V(\bar{x}) + g \sum_{k=2}^{N} \left(m_k + \tfrac{1}{2} \right) \Omega_k(\bar{x}), \tag{3.32b}$$

where m_k are the quantum numbers of the transverse excitations.

3.4. THE SEPARATION OF TIME SCALES

Here we discuss a method which can be used to handle a tunneling problem in a real physical system of many coupled degrees of freedom. The classical dynamics in such a problem will generally be too complicated to calculate explicitly. However, in many cases the important part of configuration space can be effectively reduced to only a few degrees of freedom. This reduction is performed by a *separation of time scales*, and we examine the situations which allow us to carry it out. This analysis was introduced by Sethna [3] in his treatment of tunneling centers coupled to phonons.

Suppose we can identify a tunneling coordinate, x, which is coupled to many modes. We wish to separate the modes into 3 categories according to their small oscillation frequencies ω_k: the "fast modes" $\omega_k^{(\mathrm{f})} \gg \tau^{-1}$, the "slow modes" $\omega_k^{(\mathrm{s})} \ll \tau^{-1}$, and the "important modes" $\omega_k^{(\mathrm{im})} \sim \tau^{-1}$, where the "tunneling time", τ, is the characteristic time scale of the instanton path $\bar{x}(t)$.

The fast modes, $y_k^{(\mathrm{f})}$, can be treated in the adiabatic Born-Oppenheimer approximation. They effectively renormalize the potential and mass of the tunneling coordinate and thus drop out of the problem. This was labelled the "effective mass" or the "slow-flip" approximation by Sethna in his instanton treatment of the tunneling centers in alkali halides.

On the other hand, the "slow modes", $y_k^{(\mathrm{s})}$, can be kept as frozen parameters in the tunneling calculation and thus modulate the resulting energies and tunneling matrix elements $E_n^{(i)}(y_k^{(\mathrm{s})})$ and $M_{n,n'}^{i,i'}(y_k^{(\mathrm{s})})$ respectively. The truncated hamiltonian $\overline{\mathcal{H}}$ will have residual interactions with these coordinates which can be treated for instance by perturbation theory. This scheme is known as the "Frank-Condon" approximation, and is used for example in Holstein's small-polaron treatment of the electron-phonon interactions [9]. There the electron is described by a tunneling coordinate that is fast relative to the phonon frequencies.

The important modes, $y_k^{(\mathrm{im})}$, have to be included explicitly in the computation of the tunneling matrix elements because by their very nature, if we used either of the above approximations to compute the dynamics of $y_k^{(\mathrm{im})}$, we would find large exponential errors in the computed tunneling effects.

From first inspection of the hamiltonian it is not always easy to determine which modes are relevant. In the next part, sect. 4, we shall demonstrate the subtleties involved in finding the tunneling time and the transverse frequencies in the strong coupling regime. Only after these time scales are evaluated can one argue that the effective mass or the "frozen phonon" approximations may be used. In the regions of strong coupling large renormalization effects may make the tunneling time τ and the transverse frequencies appreciably different from those of the decoupled problem. This is usually indicative of the fact that the coordinate system has not been well chosen; the coordinates do not approximate independent normal modes. When this is the case, a canonical transformation (rotation) of the coordinates will transform the problem into a more weakly coupled problem in which the relative

time scales are apparent. This regime has been labelled the "self-trapping" regime in ref. [3].

3.5. THE MULTIDIMENSIONAL TUNNELING COOK BOOK

This subsection is a summary of sect. 3. We outline in a "cook book" fashion the strategy of solving a general tunneling problem in multidimensions.

(i) Rescale distances such that all the coordinates have unit mass.

(ii) Examine the potential energy. Find the local minima and define the tunneling coordinate x to parametrize an approximate classical path between them. The projected potential $V(x)$ gives us the dimensional scales of length, time and energy, l_c, ω_c^{-1}, V_c, respectively, of the tunneling problem. $V(x)$ and these scales might be redefined after including the renormalization effects of the fast modes, and the "squeezing" effects (quantum renormalization arising from significant changes of curvatures). Evaluate the quantum parameter $g = \hbar\omega_c/V_c$; it must be considerably less than 1 (or semiclassical methods are inapplicable).

(iii) Treat the fast modes by the adiabatic approximation. This will renormalize the mass and potential of the remaining degrees of freedom which are coupled to these modes. The effects of fluctuations of these modes can also be included as potential renormalization by use of the adiabatic fluctuations approximation (AFA) described in appendix D.

(iv) Separate the slow modes. This is done by keeping them as frozen parameters in the tunneling calculation, and including them later in the truncated hamiltonian as separate modes with residual interactions which modulate the energies and tunneling matrix elements.

(v) You are left with a few important degrees of freedom. Evaluate the energies and wave functions of the low-lying states of the single well problems. (For many applications harmonic oscillator states are acceptable.)

(vi) Calculate the tunneling matrix elements $M^{i,i'}_{n,n'}(E)$ between near degenerate states. This is done in two stages:

(a) Choose two surfaces of constant wave functions in the forbidden region and find the classical path of energy $-E$ in the inverted potential that crosses the two surfaces on a perpendicular trajectory. This simultaneously defines the instanton points on both surfaces, the instanton time, and the instanton action. In general this path cannot be found analytically, but it is relatively easy to find it numerically (e.g. by variational algorithms). The instanton action and the wave functions at the instanton points determine the exponential contribution to M.

(b) Solve the $N-1$ linear second-order coupled equations of the fluctuations, eqs. (3.28), analytically, where possible, otherwise numerically.

(vii) The result of the calculation at this point is the truncated hamiltonian. The states in this hamiltonian are coupled by the tunneling matrix elements computed in (vi), and they interact with the slow modes via residual interactions. The transport

and thermodynamic properties of the system (at low temperatures) can now be calculated employing other methods. Examples for such methods are the polaronic hopping treatment of Holstein [9], and the spin coupled to a dissipative heat bath of Chakravarty and Legget [10].

4. Solutions of model problems

4.1. INTRODUCTION

In most physical systems the full multidimensional potential is not known with great quantitative accuracy. However one can learn a great deal about the behavior of these systems from a knowledge of their symmetries, energies, and time scales. Solutions of model problems are useful in this respect, as they enable us to obtain qualitative insight into the behavior of generic systems. Model problems are also useful as examples of how our method actually works.

In sect. 3 we discussed tunneling in multidimensions and we introduced the notion of "separation of time scales" as a strategy for reducing configuration space by the use of the "effective mass" or the "frozen phonon" approximations. In this section these approximations are reexamined and their domains of validity are explored. In this way, the notion of separation of time scales can be made a well-defined asymptotic expansion in terms of small adiabaticity parameters in the model problem. We shall use the PDX to solve three problems which have long been of considerable interest in various branches of physics and chemistry. We take particular care to explore the different regions of parameter spaces and to compare the complete results to those obtained using the various approximation schemes.

Each of the three problems involves a particle in a quartic double well with the coordinate x coupled to a harmonic oscillator (phonon) coordinate y. All quantities are rescaled as in subsect. 3.1. We thus consider the following potentials:

(i) The "linearly coupled" double well:

$$V_1(x, y) = \tfrac{1}{4}(x^2 - 1)^2 + \tfrac{1}{2}\omega^2 y^2 - \gamma x y + \tfrac{1}{2}\left(\frac{\gamma}{\omega}\right)^2 x^2. \tag{4.1}$$

(ii) The "gated" double well:

$$V_2(x, y) = \tfrac{1}{4}(x^2 - 1)^2 + \tfrac{1}{2}\omega^2 y^2 + \gamma(x^2 - 1)y + \tfrac{1}{2}\left(\frac{\gamma}{\omega}\right)^2 (x^2 - 1)^2. \tag{4.2}$$

The name "gated" is given for the role of the phonon coordinate as a "gate" that modulates the barrier height of the tunneling path. Linearly coupled and gated double wells are abundant in physical tunneling problems. They describe the interaction of a tunneling coordinate to first order in the phonon displacement, and thus provide the simplest possible models for coupled tunneling. Examples of problems of this sort which are extensively discussed in the literature are polaronic

conduction in insulators [9], tunneling defects in crystals [3], diffusion of light interstitials in metals [11], and the low-temperature behavior of glasses [12]. We have added counterterms to the potentials of the first two problems in order to keep the height of the adiabatic barrier (which is also the classical activation barrier), and the positions along the x-axis of the minima fixed, whilst the two parameters, the phonon frequency ω and the coupling constant γ, are varied.

(iii) The "squeezed" double well:

$$V_3(x, y) = \tfrac{1}{4}(x^2 - 1)^2 + \tfrac{1}{2}\left[\omega^2 + \gamma(x^2 - 1)^2\right] y^2. \tag{4.3}$$

This potential is quite different from the first two. The instanton path is constrained by the reflection symmetry of the potential to lie along the x-axis. However the phonon may produce large effects in the tunneling due to the "squeezing" of its curvature along the instanton path. A sizable quantum renormalization of the barrier height occurs when $g\sqrt{\gamma} \sim 1$ due to large variations in the zero-point energy of the phonon. The study of this effect takes us somewhat outside the regime of validity of the semiclassical approximation as naively applied; large fluctuation effects are incompatible with the semiclassical approximation. However, as discussed here, and in greater detail in appendix D, the problem can often be suitably renormalized so that it can be handled with the present methods. (See also [30]).

In subsect. 4.2 we start by deriving the ground state tunneling splitting of the one-dimensional quartic well, and comparing it to the result of the WKB approximation with linear turning point connections. Then we present the PDX expression for the coupled double well. In subsect. 4.3 the "effective mass" (EM) and the "frozen phonon" (FP) approximations are defined for the coupled tunneling problems. Subsect. 4.4 includes a comparison of the exact (semiclassical) results to the two approximations for the linearly coupled and gated problems. Subsect. 4.5 contains the solution of the squeezed double well and the quantum renormalization of the potential. Also, we discuss the use of the adiabatic fluctuations approximation to describe this phenomenon.

4.2. THE PDX RESULTS

First we derive the PDX expression for the ground-state splitting of the 1-dimensional (decoupled) double well. The quartic potential is

$$V(x) = \tfrac{1}{8}\omega_1^2(x^2 - 1)^2, \tag{4.4}$$

with minima at $x_m^{\pm 1} = \pm 1$. The restricted ground state of the right well ($x_m = 1$)

evaluated at a decomposition point $x_d = 1 - d$, where $\sqrt{g/\omega_1} \ll d \ll 1$, is

$$\psi_0^{(1)}(x_d) = \left[\frac{\omega_1}{\pi g}\right]^{1/4} \exp\left[-\frac{\omega_1}{2g} d^2\right], \tag{4.5}$$

and its energy is $E_0^{(1)} = \frac{1}{2}g\omega_1$. The tunnel splitting of the ground-state energy of the double well problem is

$$E_0^{\pm} = E_0^{(1)} \pm \Delta, \tag{4.6}$$

where Δ is equal to the tunneling matrix element $M_{0,0}(\frac{1}{2}g\omega_1)$ of eqs. (3.31). Thus

$$\Delta/g = v(x_d)\left[\psi_0^{(1)}(x_d)\right]^2 \exp\left[-\frac{1}{g} W(-x_d, x_d, \tfrac{1}{2}g\omega_1)\right]$$

$$= \left[\frac{\omega_1}{\pi g}\right]^{1/2} v(x_d) \exp\left[-\frac{1}{g} W(-1,1,0) + \tfrac{1}{2}\omega_1 T(-x_d, x_d, 0)\right]\left[1 + O\left(\frac{g\omega_1}{V(x_d)}\right)\right], \tag{4.7a}$$

where, in the second line, the action W has been expanded to first order in the energy:

$$W(a, b, E) = \int_a^b dx \sqrt{2(V(x) - E)}\,, \tag{4.7b}$$

$$T = \frac{\partial W}{\partial E}\,. \tag{4.7c}$$

The classical path which contributes to $W(a, b, 0)$ is the *zero* energy path and not the original instanton path of energy $-E_0^{(1)}$. This choice of path, which for simplicity we shall also call the instanton path, simplifies the following calculations and will be used throughout this section of the paper. In eq. (4.7a), we use the harmonic approximation for the dynamics of the (zero-energy) instanton path near ± 1 to permit the substitution $\omega_1 d^2 + W(-x_d, x_d, 0) = W(-1, 1, 0)[1 + O(d)]$. We can also express the velocity $v(x_d)$ in terms of the velocity at the classical turning point $x_{tp} = 1 - \sqrt{g/\omega_1}$; $v(x_{tp}) = \sqrt{g\omega_1}$:

$$v(x_d) = \sqrt{g\omega_1}\, e^{\omega_1 T(x_{tp}, x_d, 0)}. \tag{4.8}$$

Combining and evaluating eqs. (4.7b) and (4.7c) we arrive at

$$\frac{\Delta}{g} = \omega_1 \left[\frac{2\omega_1}{\pi g}\right]^{1/2} \exp\left[-\frac{2\omega_1}{3g}\right]. \tag{4.9}$$

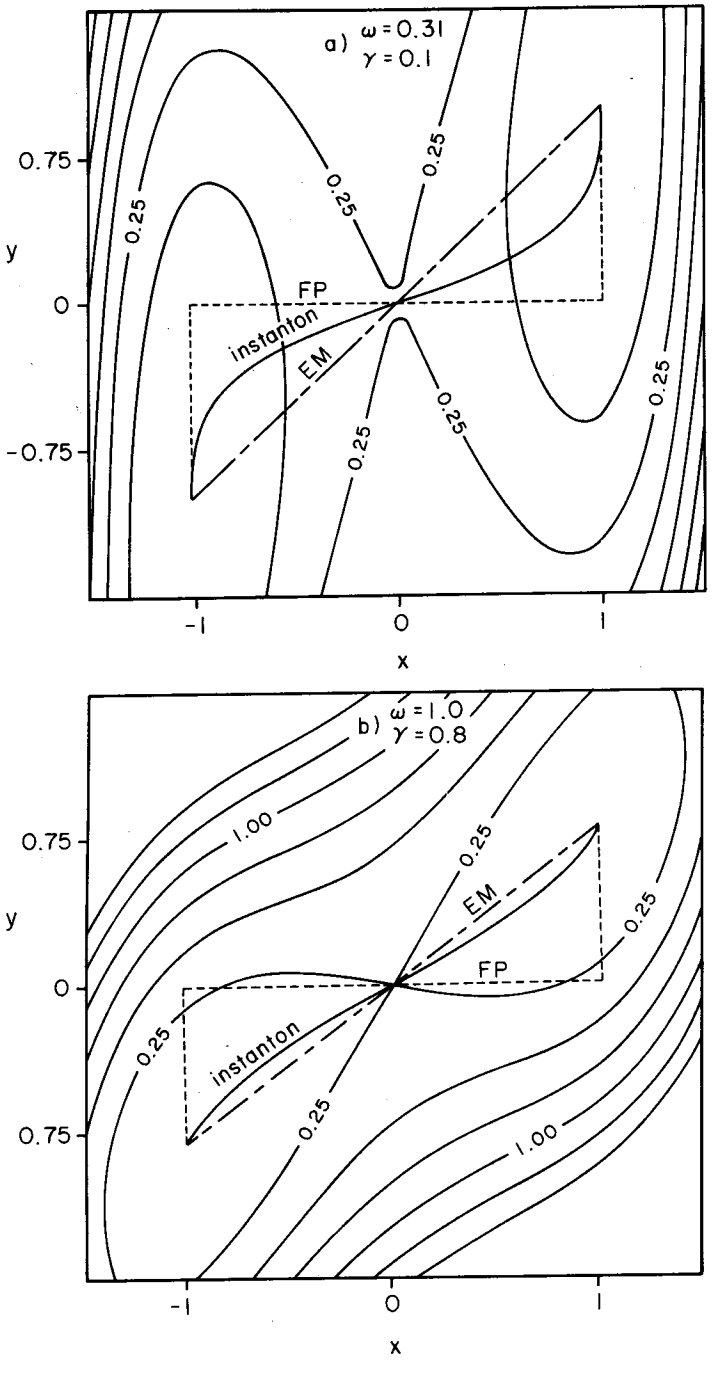
a) ω = 0.31
γ = 0.1
0.25
0.25
0.25
0.25
0.25
0.25
FP
instanton
EM
0.75
0
-0.75
y
-1
0
1
x
b) ω = 1.0
γ = 0.8
1.00
0.25
EM
0.25
FP
0.25
instanton
0.25
1.00
0.75
0
0.75
y
-1
0
1
x

Fig. 8.

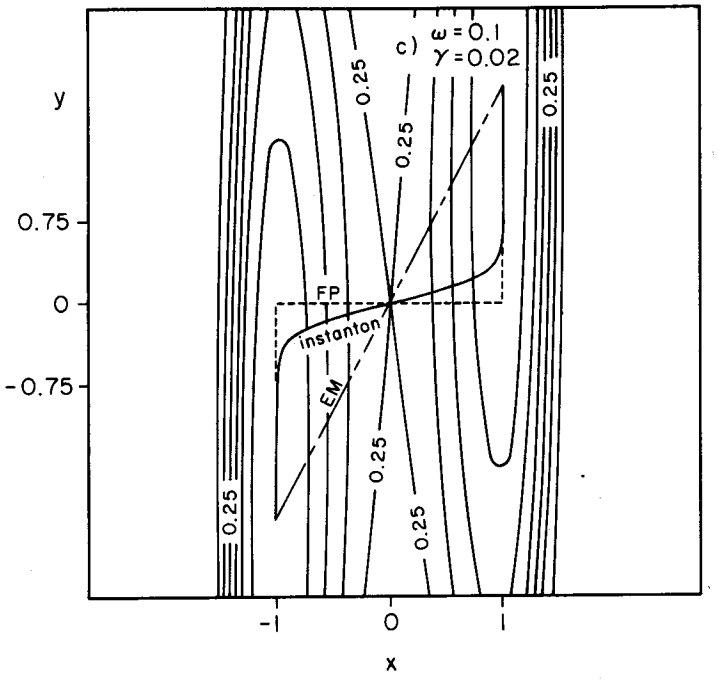

Fig. 8. The linearly coupled double well. The potential $V_1(x, y)$ of eq. (4.1) and the instanton path (solid line), are drawn for three values of γ and ω. The long-short dashed line marks the adiabatic path, which is used in the EM approximation, and the short-dashed line marks the FP path. The tunnel-splitting Δ is given in units of $\sqrt{g}$. The parameters and tunnel-splittings for the three potentials are (a) $\omega = 0.316$, $\gamma = 0.1$, $\Delta^{EM} = 1.7\exp[-1.33/g]$, $\Delta^{FP} = 2\exp[-1.37/g]$, $\Delta = 1.8\exp[-1.16/g]$. (b) $\omega = 1$, $\gamma = 0.8$, $\Delta^{EM} = 2\exp[-1.22/g]$, $\Delta^{FP} = 2.3\exp[-2.04/g]$, $\Delta = 2.3\exp[-1.18/g]$. (c) $\omega = 0.1$, $\gamma = 0.02$, $\Delta^{EM} = 1.3\exp[-2.10/g)$, $\Delta^{FP} = 1.9\exp[-1.40/g]$, $\Delta = 1.3\exp[-1.27/g]$.

This is the correct semiclassical expression for Δ (see ref. [19]). It is instructive to compare eq. (4.9) to the result one would get by using the WKB method with a linear turning point connection formula

$$\Delta^{ltp}/g = \tfrac{1}{2}e^{-1}\omega_1 \exp\left[-\frac{1}{g}\int_{\sqrt{g/\omega_1}-1}^{1-\sqrt{g/\omega_1}} dx\sqrt{2\left(V(x)-\tfrac{1}{2}g\omega_1\right)}\right]. \tag{4.10}$$

By evaluating eq. (4.10) explicitly, one can verify that the error introduced by the use of a linear turning point formula for the ground state is a factor of $[\pi/e]^{1/2}$. (This result is traceable to Goldstein [13].)

The 2-dimensional (coupled) problems of eqs. (4.1)–(4.3) are solved numerically. There are two quantities we need to compute separately when the quantum parameter, g, is free: the prefactor A, and the exponent $\overline{W}$, such that the ground-state tunnel splitting is

$$\frac{\Delta}{g} = \frac{A}{\sqrt{g}}\exp\left[-\frac{\overline{W}}{g}\right]. \tag{4.11}$$

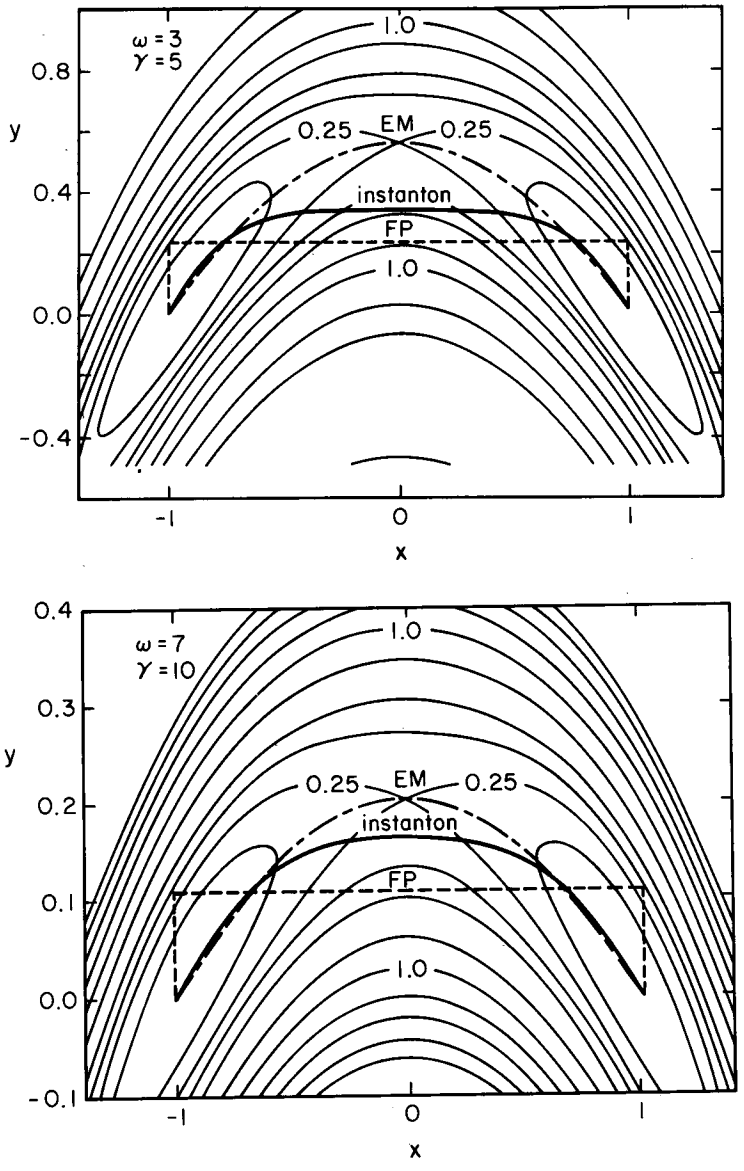

Fig. 9. The gated double well. The potential $V_2(x, y)$ of eq. (4.2) and the instanton path (solid line) are drawn for three values of γ and ω. The dotted-dashed line marks the adiabatic path, which is used in the "effective mass" approximation, and the dotted line marks the "frozen phonon" path. The parameters (γ, ω), and the exponential contributions (W) to the tunnel-splittings are (a) $\omega = 3$, $\gamma = 5$, $W^{EM} = 1.84$, $W^{FP} = 1.75$, $\overline{W} = 1.47$. (b) $\omega = 7$, $\gamma = 10$, $W^{EM} = 1.21$, $W^{FP} = 1.44$, $\overline{W} = 1.15$. (c) $\omega = 1.5$, $\gamma = 2$, $W^{EM} = 2.20$, $W^{FP} = 1.62$, $\overline{W} = 1.48$.

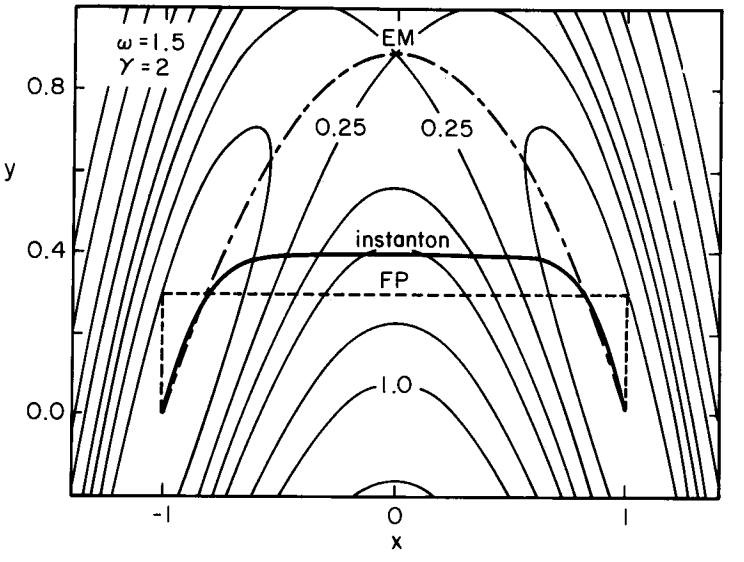

Fig. 9 (continued).

Both these quantities are uniquely determined by the instanton path $(x, \bar{y}(x))$. Again, it is the classical path of zero energy in the inverted potential (just as in the decoupled case) that goes between the two minima at $x = \pm 1$. It can be found by the use of Jacobi's form of the least action principle [14], which is

$$\delta_\alpha W = \frac{\partial}{\partial \alpha} \int_{-1}^{+1} \mathrm{d}x \sqrt{2(M_\alpha(x) V(x, y_\alpha(x))}\Big|_{y_\alpha(x)=\bar{y}(x)} = 0, \tag{4.12}$$

where $M_\alpha(x)$ is the path's length increment or "effective mass"

$$M_\alpha(x) = 1 + \left(\frac{\mathrm{d}y_\alpha}{\mathrm{d}x}\right)^2. \tag{4.13}$$

In practice, the minimization of W requires very few variational parameters for the trial paths $y_\alpha(x)$ since the instanton path is smooth and well behaved, as is demonstrated in figs. 8 and 9. After obtaining the instanton action, which is the exponent $\overline{W}$, we choose x_d close to 1 as the decomposition point, and calculate the velocity $v(x_\mathrm{d})$ and time $T(-x_\mathrm{d}, x_\mathrm{d}, 0)$. We find the eigenvalues ω_a^2, ω_b^2, of the quadratic minimum, and use the appropriate harmonic oscillator ground-state wave functions. Λ of eq. (3.30) is computed by numerical integration of the one-dimensional fluctuation equations (3.27), using a Runga-Kutta algorithm. Thus the final expression for Δ is

$$\Delta/g = \Lambda \left[\frac{\omega_a \omega_b}{\pi g}\right]^{1/2} \exp\left[-\frac{1}{g}\int_{-1}^{+1} \sqrt{2M(x)V(x, \bar{y}(x))} + \tfrac{1}{2}(\omega_a + \omega_b)T\right]. \tag{4.14}$$

Pictures of the instanton paths for various choices of parameters, as well as the values of the exponents and prefactors, are presented in figs. 8 and 9.

4.3. THE EFFECTIVE MASS AND FROZEN PHONON APPROXIMATIONS

The effective mass (EM) approximation entails approximating the instanton path by the adiabatic path $(x, y^{\mathrm{ad}}(x))$ where

$$\left.\frac{\partial V(x,y)}{\partial y}\right|_{y=y^{\mathrm{ad}}(x)} = 0. \tag{4.15}$$

Thus the potential can effectively be replaced by the renormalized potential

$$V^{\mathrm{ad}}(x) = V(x, y^{\mathrm{ad}}(x)), \tag{4.16}$$

and the mass by the renormalized effective mass

$$M^{\mathrm{ad}}(x) = 1 + \left(\frac{\mathrm{d}y^{\mathrm{ad}}}{\mathrm{d}x}\right)^2. \tag{4.17}$$

This results in an effective one-dimensional problem which can be easily solved to obtain the tunneling rate. In the linearly coupled double well the EM approximation gives for the tunnel splitting

$$\Delta^{\mathrm{EM}} = \sqrt{2}\left[\frac{2\sqrt{2}}{\pi g\sqrt{M^{\mathrm{ad}}}}\right]^{1/2} \exp\left[-\frac{2\sqrt{2M^{\mathrm{ad}}}}{3g}\right], \tag{4.18a}$$

where

$$M^{\mathrm{ad}} = 1 + \left(\frac{\gamma}{\omega^2}\right)^2. \tag{4.18b}$$

In figs. 8 and 9 the short-long dashed lines are the adiabatic paths, and by comparing them to the true instanton paths it is clear that this approximation is good only in a certain regime of the potential parameters.

The frozen phonon FP approximation is obtained by freezing the coordinate $y = \mathrm{const}$, and thus approximating the instanton path by a straight path (x, y), $-1 < x < 1$. The tunneling splitting is thus

$$\Delta^{\mathrm{FP}}/g = \int_{-\infty}^{\infty} \mathrm{d}y\, \phi_0(y - y_{\mathrm{m}}^{+})\phi_0(y - y_{\mathrm{m}}^{-})\Delta^{\mathrm{b}}(y), \tag{4.19}$$

where $(\pm 1, y_{\mathrm{m}}^{\pm})$ are the two minima, and $\Delta^{\mathrm{b}}(y)$ is the "bare" tunneling splitting of

the one-dimensional problem of unit mass and "bare" potential $V(x|y)$:

$$V(x|y) = V(x, y). \tag{4.20}$$

ϕ_0 is the relaxed ground-state wave function of the phonon. Integration of eq. (4.19) by steepest descent results in

$$\Delta^{\mathrm{FP}}/g = \mathrm{e}^{-P(\bar{y})}\Delta^{\mathrm{b}}(\bar{y}), \tag{4.21}$$

where $\bar{y}$ is the most dominant contribution (saddle point) to eq. (4.19), and P is the

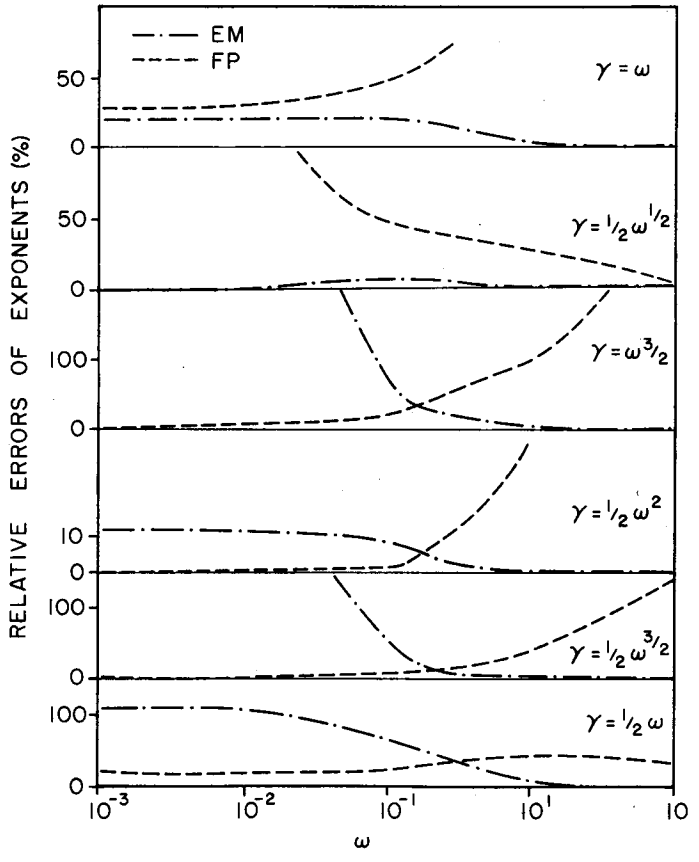

Fig. 10. The linearly coupled double well. The relative errors $(W - \overline{W})/\overline{W}$ in the exponents of the "effective mass" (EM), and "frozen phonon" (FP) approximations. Different cuts in the parameter space, $\gamma(\omega)$, are sampled.

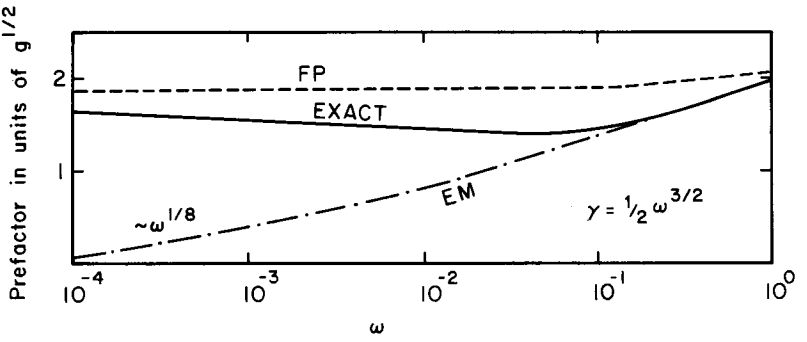

Fig. 11. The linearly coupled double well. The prefactor A of eq. (4.11), for the line $\gamma = \frac{1}{2}\omega^{3/2}$ in the parameter space of V_1. The prefactor varies smoothly between the "effective mass" (EM) and "frozen phonon" (FP) approximations.

phonon overlap exponent

$$P(\bar{y}) = \frac{1}{2g}\omega\left[(\bar{y} - y_{\mathrm{m}}^{+})^2 + (\bar{y} - y_{\mathrm{m}}^{-})^2\right]. \tag{4.22}$$

The dominant paths in the FP approximation are shown by short dashed lines in figs. 8 and 9. The vertical segments contribute to the overlap factor of eq. (4.22). Again it is clear by inspection when the approximation is valid.

The accuracy of the two approximations in various regions of parameter space is summarized in figs. 10–13.

4.4. THE LINEARLY COUPLED AND THE GATED DOUBLE WELLS

The linearly coupled double well, eq. (4.1), and the gated double well, eq. (4.2), exhibit different reflection symmetries on the x- and y-axis. However, they share the property that the instanton paths in both models generally bend in the two-dimensional space and thus have complicated dynamics. If the phonon coordinate is integrated out of the path integral, as in the treatment of ref. [3], the instanton equation of motion contains a term which is non-local in time called the time-retarded interaction (ref. [4], p. 234), which reflects this complexity.

We scan the parameter spaces (ω, γ) and compare the PDX tunneling exponent $\overline{W}$, which is the action of the instanton path, to the approximated exponent, given by the action of the EM and FP paths. Fig. 10 exhibits the relative errors of the two approximations for the linearly coupled model. Note that both approximations always *overestimate* the exponent. This is a result of the variational principle eq. (4.12). We can map the regimes of validity in the parameter space. This is done in figs. 12 and 13. The solid lines in the figures mark the boundaries of the regions of parameter space where the specified approximation is accurate to better than 10 per

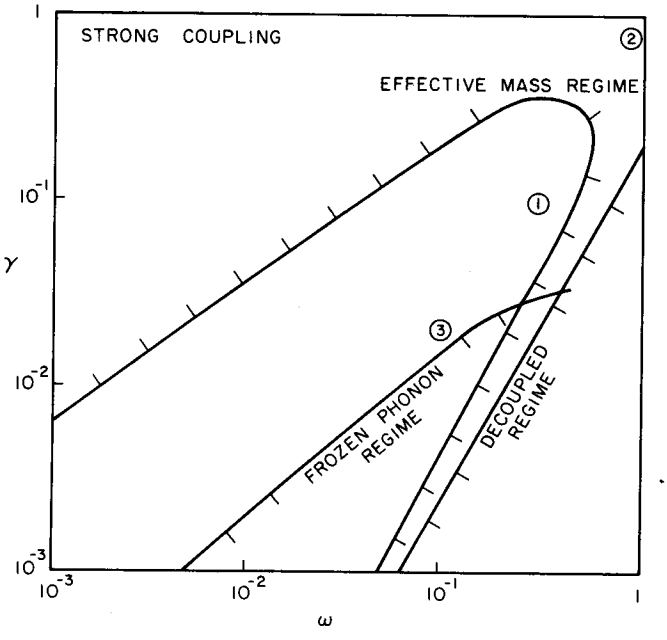

Fig. 12. The linearly coupled double well. The regimes of validity (relative errors less than 10 per cent) of the "effective mass" and "frozen phonon" approximations are charted in the (γ, ω) space. The points 1, 2 and 3 are the values of the parameters in figs. 8a, b and c respectively.

cent. We have also computed the prefactors of the linearly coupled problem along the line $\gamma = \frac{1}{2}\omega^2$, and compared it to the corresponding EM and FP expressions. We find that no dramatic behaviour of the prefactor occurs and in most cases a careful calculation is unnecessary.

Figs. 8 and 9 provide examples of the potentials and instanton paths in the different regimes of parameter spaces for the linearly coupled and the gated model problems respectively. One can picture the instanton path as the path in which a ball of zero energy would roll from one maximum to the other in the inverted potential. The two other paths represent trial paths corresponding to the EM and FP approximations, and they produce actions which vary in degree of accuracy as we vary ω and γ.

We can regard the regimes of the two approximations in the context of the separation of time scales that was discussed in subsect. 3.4. The EM regime is valid when the instanton path is close to the adiabatic path, hence we can effectively separate the transverse mode (fluctuation) as being "fast" compared to the tunneling coordinate. Note, in fig. 12, that in the strongly coupled $(\gamma > \omega)$ regime, the transverse mode can be fast even when $\omega \ll 1$. The strong coupling distorts the potential such that the characteristic tunneling time is increased and becomes

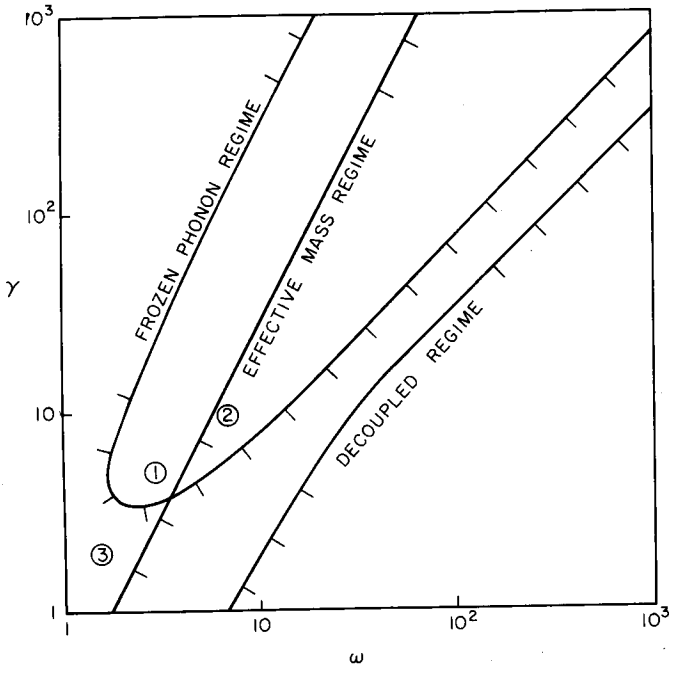

Fig. 13. The gated double well. The regimes of validity (relative errors less than 10 per cent) of the "effective mass" and "frozen phonon" approximations are charted in the (γ, ω) space. The points 1, 2 and 3 are the values of the parameters in figs. 9a, b and c respectively.

substantially larger than ω^{-1}. It is then useful to rotate in the (x, y) plane and solve a weakly coupled problem in the EM approximation.

On the other hand, the FP is valid when it is safe to separate the low-frequency phonon from the tunneling calculation by freezing it. The region of parameter space that lies outside both the EM and FP regimes is where the time scales cannot be separated, and both approximations fail badly. In this regime, a full calculation of the instanton path dynamics is essential in order to obtain a reasonably accurate answer.

4.5. THE SQUEEZED DOUBLE WELL

The squeezed double well possesses a reflection symmetry $y \to -y$. This forces the instanton path to lie on the x-axis (see fig. 14a). Thus the *naive* calculation of the exponent in eq. (4.14) would use the bare potential $V^{b}(x) = V_3(x, 0)$ and the instanton path $\bar{x}(t)$. The term "naive" will be explained shortly. The result would be

$$\Delta = \Delta^{b} \exp\left[-\tfrac{1}{2}(\nu(T) - \omega)T\right], \tag{4.23}$$

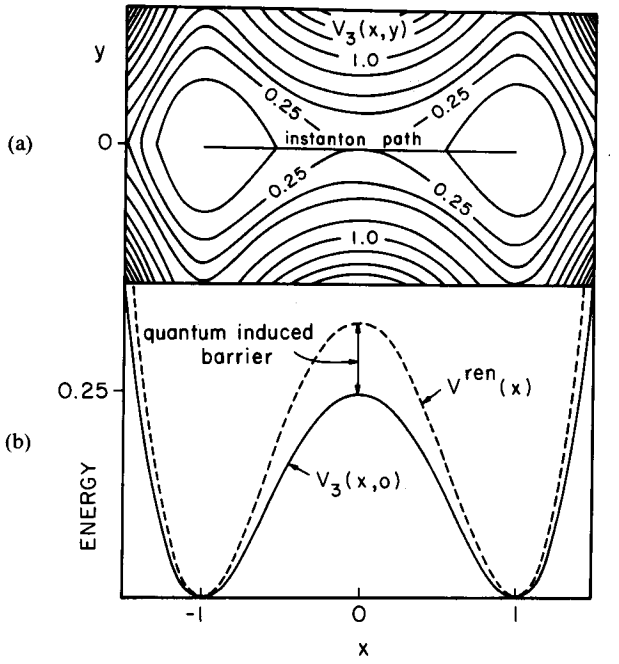

Fig. 14. The squeezed double well. The potential $V_3(x, y)$ of eq. (4.3) is plotted for $\omega = 2$, $\gamma = 10$. (a) The potential $V_3(x, y)$ of eq. (4.3) and instanton path (solid line) in the (x, y) plane. (b) The bare potential $V_3(x,0)$ (solid line) and the renormalized potential $V^{\text{ren}}(x)$ (dashed line) of eq. (4.27) for the case where the quantum parameter g is 0.1.

where Δ^b is the "bare" tunneling splitting given by solving the one-dimensional problem as in subsect. 4.2, eq. (4.9), using the bare 1D potential $V^b(x) = V_3(x,0)$, and T is the time between the two turning points defined prior to eq. (4.8):

$$T = \sqrt{\tfrac{1}{2}} \log\left[\frac{2\sqrt{2}}{g}\right]. \tag{4.24}$$

ν is the stability frequency obtained from the solution of the fluctuation equation:

$$\nu(T) = \log[q(T)]/T, \tag{4.25}$$

where

$$\ddot{q}(t) = \Omega^2(t) q(t), \tag{4.26a}$$

with

$$\Omega^2(t) = \omega^2 + \gamma\left(\bar{x}^2(t) - 1\right)^2, \tag{4.26b}$$

subject to the initial conditions

$$q(0) = 1, \qquad \dot{q}(0) = \omega. \tag{4.26c}$$

This "naive" approach is valid so long as $g\nu(T)T \ll 1$. If, on the other hand, $g\nu(T)T$ is *not* small, then the path integral is not dominated by paths in the neighborhood of the "bare" instanton path. While it is still true that the instanton path has the smallest action, the large value of the stability angle $g\nu(T)T$ implies that there are very few paths in the neighborhood of similarly small action. Rather, the largest contribution to the path integral comes from the vicinity of that path which minimizes the quantity $W + \frac{1}{2}g\nu(T)T$. Since $\nu(T)$ is dependent on the path this leads us, in general, to a self-consistent problem of great complexity. Moreover, since $g\nu(T)T$ is explicitly proportional to the *quantum* parameter g, one might expect that the semiclassical approximation itself is invalid unless this quantity is small.

In the remainder of this section we will show how semiclassical methods can be applied to the squeezed double well even when the naive approach is invalid. We use in this approach to the problem the adiabatic fluctuation approximation (AFA), which is discussed in detail in appendix D. In spirit, our approach is similar to that of Coleman and Weinberg [15]. It is based on the observation that when the characteristic frequencies of the transverse fluctuations are large compared to the inverse tunneling time, their effect can be absorbed into a local (in the tunneling coordinate) renormalization of the potential that appears in the instanton action. In the context of the squeezed double well, this means that the tunneling problem can be treated as strictly one-dimensional, but with the renormalized potential

$$V^{\mathrm{ren}}(x) = V_3(x,0) + \tfrac{1}{2}g\left\{\left[\omega^2 + \gamma(x^2-1)^2\right]^{1/2} - \omega\right\} \tag{4.27}$$

appearing in the action in place of $V_3(x,0)$. Hence, the tunnel splitting is

$$\Delta^{\mathrm{AFA}} = \Delta^{\mathrm{b}}(V^{\mathrm{ren}}). \tag{4.28}$$

This is illustrated in fig. 14b for $g = 0.1$. (Note that the potential renormalization is just due to the instanton zero-point energy $\frac{1}{2}g\Omega(x)$, of the transverse y-motion. This generalizes to potentials which are nonquadratic in the y-direction.)

The AFA would be exact if the coefficient Ω^2 for the transverse fluctuations in eq. (4.26a) were time independent. Thus in the present model, the AFA produces errors which vanish (exponentially) as the parameter $\alpha \to 0$, where

$$\alpha = \langle \dot{\Omega}/\Omega^2 \rangle . \tag{4.29}$$

Here $\langle\ \rangle$ stands for typical-value-of, and $\Omega = \Omega(x^{\mathrm{ren}}(t))$, where x^{ren} is the classical path in the renormalized potential. Since $\Omega \sim \sqrt{\omega^2 + \gamma}$ and $\dot{x} \sim 1$, α is small over a wide range of parameter space. In particular, whenever a sizeable potential renormalization is produced, that is whenever $g[\Omega - \omega] \gtrsim 1$, the condition $g \ll 1$ necessarily implies that $\alpha \ll 1$. Note that in this regime, calculations based on the unrenormalized instanton path can even be *qualitatively* wrong. In particular there are cases where the squeezing effect provides most, or all, of the tunnel barrier! This

is an example of dynamically induced barrier formation. It can produce interesting physical phenomena such as an anomalous mass dependence of the tunnel splitting. We are currently applying some of the results discussed here to the problem of hydrogen diffusion on metal surfaces [16].

5. Summary and future applications

In sect. 2 we introduced a quantum-mechanical technique called the path decomposition expansion (PDX). The PDX can be used to break configuration space up into overlapping restricted regions, and to construct a direct sum representation of the full hamiltonian. This enables us to study multidimensional tunneling problems that break up naturally into weakly coupled wells. The semiclassical approximation is closely tied to the PDX approach, since by using it we can obtain non-perturbative effects of tunneling through the barrier regions. The tunneling matrix elements can be calculated to leading order in the quantum parameter and divergences in the prefactor can be avoided by choosing the decomposition surfaces away from classical turning points.

A previous generalization of the WKB method to multidimensions was carried out by Banks, Bender and Wu [17]. They formulated a connection procedure of the multidimensional wave function to the exponentially decaying solution in the forbidden region and arrived at the same fluctuation equation as eqs. (3.27). Their answer differs from eqs. (3.25) only by some undetermined constants. The other commonly used techniques for solving multidimensional tunneling problems are mainly based on the instanton formalism (refs. [18,19,31]). There, the ground-state tunneling effects are derived from the contribution of the classical path of zero energy and infinite imaginary time through the forbidden region. Since it contains little information about the classically allowed regions, the instanton method does not lend itself to problems involving tunneling from initially excited states of the potential wells, nor to problems in which back-scattering effects are significant (i.e. the effect of spectrum of final states). In one dimension, these difficulties have been elegantly surmounted by a related method involving summing over complex-time classical paths [20]. An additional difficulty of the instanton formalism is that the prefactor, which in complicated potentials involves a ratio of infinite determinants, is difficult to compute. (Such a computation was successfully carried out by Chang and Chakravarty [21].) On the other hand, the instanton formalism is more adequate than the PDX for solving problems where there is a continuum of weakly coupled modes whose time scales cannot be directly separated from the tunneling time, as in the problem of a macroscopic tunneling coordinate coupled to a heat bath [22]. The instanton formalism allows us to map the tunneling problem into a truncated problem, even though no real separation of time scales exists. See refs. [23,24].

In conclusion to this paper, we briefly outline some future applications of the PDX technique to tunneling problems.

In ref. [25] it was shown that it is possible to map an optical transition rate problem into a multidimensional tunneling problem, and that in particular, the subgap photogeneration of soliton-antisoliton pairs in polyacetylene can be understood in this way. Polyacetylene is a half-filled Peierls system which is fairly accurately described by the continuum (field-theory) model of TLM [26]. Thus the subgap optical absorption is seen to be a direct experimental probe to the contribution of large amplitude (non-perturbative) fluctuations of the field to the current-current correlation function of a simple field theory. In ref. [25] a crude estimate of the magnitude of this effect was obtained by guessing an approximate instanton path. Since there are now a fair number of experiments which are in good qualitative agreement [27] with the results of ref. [25], it seems appropriate to obtain more quantitatively reliable results. The exact time-dependent classical solutions of the field equation are not known analytically. However, we can obtain good results by minimizing the action variationally, and using the AFA to calculate the prefactor.

Another system in which the potential is known with high enough accuracy that a detailed calculation seems worthwhile, and in which interesting experimental results have been found, is the problem of hydrogen diffusion on the surfaces of metals. At low temperatures, a temperature-independent diffusion rate with an anomalous isotope dependence has been observed [28]. We [16] are currently computing the diffusion rate directly from the computed potential. Preliminary results indicate that "squeezing" effects, i.e. quantum renormalization of the potential, are important in understanding the isotope dependence.

The "squeezing" effect, calculated in the adiabatic fluctuations approximation (AFA) in subsect. 4.5, generalizes in a field theory to the effective potential given by the 1-loop approximation. In some field theories, for example massless scalar electrodynamics [15], this term dynamically creates a double well problem and causes a spontaneous symmetry breaking. We expect the PDX technique to be a useful tool in calculating tunneling amplitudes between the vacua [29], [30].

We wish to thank L.S. Schulman and J. Sethna for their helpful suggestions and comments. This work was supported in part by a National Science Foundation grant no. NSF-DMR-8318051, and one of us (S.K.) would like to thank the Alfred P. Sloan foundation for a fellowship.

Appendix A

THE PDX: 1D EXAMPLES

In this appendix we shall first demonstrate the use of the single surface PDX, eq. (2.17), with two simple examples in one dimension: the free Green function and the infinite square well (ISW). Then we shall calculate the energy levels of the ISW using the 2-site PDX and the direct-sum representation of the hamiltonian. This is an

important example of the direct-sum representation, since all the restricted regions are classically allowed ($V(x) < E$), and the transition matrix elements are not small and strongly E-dependent. Thus, this problem indicates that the PDX could possibly be applied to other non-tunneling problems.

First, let us consider the "free" Green function (no potential energy)

$$G(x_1, x_2, E) = i\frac{m}{k}\exp\left[-i\frac{k|x_2 - x_1|}{\hbar}\right], \tag{A.1}$$

where

$$k = \sqrt{2mE}\,. \tag{A.2}$$

Let us pick x_1, x_2, r such that $x_1 < r < x_2$, so r is our "surface" of decomposition. The restricted Green function to the right of r, G^r (which can be found for example by the "method of images" [6]) is

$$G^r(x, x_2, E) = -\frac{2m}{k}\sin\left(\frac{k(x-r)}{\hbar}\right)\exp\left[-i\frac{k(x_2-r)}{\hbar}\right]. \tag{A.3}$$

It is then easy to verify that G and G^r satisfy the PDX equation

$$G(x_1, x_2, E) = G(x_1, r, E)\left(-\frac{\hbar}{2m}\right)\frac{\partial}{\partial x}G^r(x, x_2, E)\bigg|_{x=r}. \tag{A.4}$$

The second example is the ISW, where $V(x) = 0$ for $0 < x < L$, and $V(x) = \infty$ elsewhere. We choose the decomposition "surface" at a point r in the well, $0 < x_1 < r < x_2 < L$, and verify eq. (A.4) using

$$G(x_1, x_2, E) = -\frac{2m}{k\sin(kL/\hbar)}\sin\left(\frac{kx_1}{\hbar}\right)\sin\left(\frac{k(L-x_2)}{\hbar}\right), \tag{A.5}$$

$$G^r(x, x_2, E) = -\frac{2m}{k\sin(k(L-r)/\hbar)}\sin\left(\frac{k(x-r)}{\hbar}\right)\sin\left(\frac{k(L-x_2)}{\hbar}\right). \tag{A.6}$$

Note the appearance of the "fictitious" poles of G^r on the right-hand side of eq. (A.4) at

$$\tilde{E}_n^r = \frac{n^2\pi^2\hbar^2}{2m(L-r)^2}, \qquad n = 1, 2, \ldots, \tag{A.7}$$

that is to say, poles that do not belong to G. These make no contribution to the PDX

since $G(x, r, \tilde{E}_n^r)$ vanishes. This teaches us to use considerable caution when studying the analytic structure of a Green function from a PDX expression.

We would like to use this opportunity to demonstrate the fact that the symmetric form of the PDX is satisfied by other restricted Green functions, explicitly considering the function $\tilde{G}^r$ that satisfies the "log-derivative" or "emitting" boundary conditions

$$\frac{\partial}{\partial x}\log\tilde{G}^r(x,x',E)\bigg|_{x=r} = \frac{i}{\hbar}\sqrt{2m(E-V(r))} = \frac{ik}{\hbar}. \tag{A.8}$$

These boundary conditions yield instead of the two "Dirichlet" restricted Green functions (A.3) and (A.6), the functions

$$\tilde{G}^r = i\frac{k}{m}\exp\left[-i\frac{k(x_2-x)}{\hbar}\right], \tag{A.3'}$$

$$\tilde{G}^r = i\frac{m}{k}\left[\exp\left[-i\frac{k(x_2-x)}{\hbar}\right] - \exp\left[-i\frac{k(2L-x_2-x)}{\hbar}\right]\right], \tag{A.6'}$$

respectively. It is easily verified that these functions indeed satisfy eq. (2.17). Notice, unlike G^r in eq. (A.6), $\tilde{G}^r$ in eq. (A.6') has no spurious poles.

Let us now consider the ISW of eq. (A.5) and set $\hbar = m = 1$. We divide the well into three regions (see fig. 15) by two decomposition surfaces at a and $a+b$ such that $2a+b=L$. The two-site Green functions $G^{(1)}$ and $G^{(2)}$ have identical poles (as a result of the symmetry of the surfaces) at $E_n^{(1)}$:

$$E_n^{(1)} = \frac{n^2\pi^2}{2(a+b)^2}, \qquad n = 1,2,\ldots, \tag{A.9}$$

$$G^{(1)}(x,x',E) = \frac{-2}{a+b}\sum_n \frac{\sin(n\pi x/(a+b))\sin(n\pi x'/(a+b))}{E-E_n^{(1)}}$$

$$= \frac{-2}{k}\frac{\sin(kx)\sin(k(a+b-x'))}{\sin(k(a+b))} \qquad \text{for } x' > x. \tag{A.10}$$

The transition matrix (eq. (2.33)) is

$$M_{n,n'}(E) = \frac{-k}{(a+b)\sin(k/b)}\sin\left(n\pi\frac{a}{a+b}\right)\sin\left(n'\pi\frac{a}{a+b}\right), \tag{A.11}$$

where k is defined in eq. (A.2).

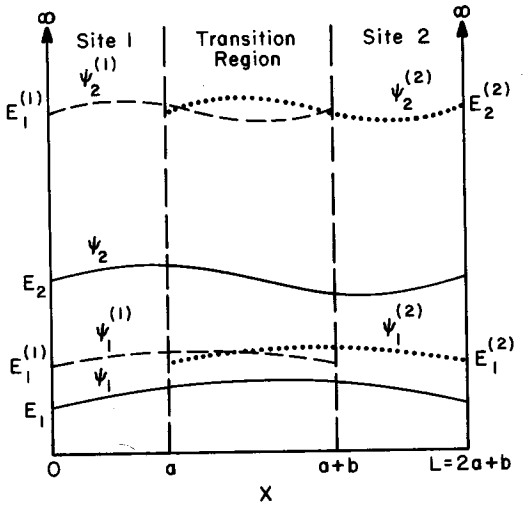

Fig. 15. The 2-site decomposition of the ISW problem. The two decomposition surfaces are drawn and the lowest two states of $G^{(1)}$, $G^{(2)}$ and G are represented schematically by the dashed, dotted and solid lines respectively. $E_n^{(1)}$ and E_m are defined in eqs. (A.9) and (A.13) respectively.

Solving eq. (2.37) requires finding the energies E_m and nullifying vectors (a_n^m, b_n^m), $n = 1, 2, \ldots, \infty$, such that

$$\left(E_m - E_n^{(1)}\right) a_n^m + \sum_{n'} M_{n,n'}(E_m) b_{n'}^m = 0,$$

$$\sum_{n'} M_{n,n'}(E_m) a_{n'}^m + \left(E_m - E_n^{(1)}\right) b_n^m = 0. \tag{A.12}$$

The solutions for these energies are

$$E_m = \frac{m^2 \pi^2}{2(2a+b)^2}, \qquad m = 1, 2, \ldots. \tag{A.13}$$

Using eq. (A.10) one can verify directly that the corresponding vectors are

$$a_n^m = \frac{\sin(n\pi a/(a+b))}{E_m - E_n^{(1)}}, \qquad b_n^m = (-1)^{m+1} a_n^m. \tag{A.14}$$

Thus the wave functions of the full ISW $\psi_m(x)$ can be expressed in terms of the restricted states $\psi_n^{(i)}$, $i = 1, 2$ as

$$\psi_m(x) = \sum_n a_n^m \psi_n^{(1)}(x) + b_n^m \psi_n^{(2)}(x). \tag{A.15}$$

Accidental degeneracies occur when a/b is a rational number. In that case $M_{n,n'}(E)$ may have a pole at E_m and eq. (A.12) is not well defined. One should then first lift the degeneracy by moving the surfaces an infinitesimal distance δ, and then calculate the solutions of eq. (A.12) to lowest order in δ.

Appendix B

THE PREFACTORS OF THE SEMICLASSICAL APPROXIMATION

In subsect. 3.3 we encountered two prefactor expressions, Λ_n in eqs. (3.25) and $\Lambda_{n,n'}$ in eqs. (3.29), which are the results of the semiclassical approximation to the wave function ψ_n and the tunneling matrix element $M_{n,n'}$ respectively. These expressions are given in a form that does not manifestly show their relation to the classical dynamics of the instanton path. In this appendix we derive the alternate expressions, eqs. (3.28) and (3.30), which define the prefactors in terms of the classical fluctuations about the instanton path. We shall soon transform the ratios of determinants in eqs. (3.25) and (3.29) to determinants of solutions to linearized initial value problems which are the stability equations of the instanton path. This derivation is analogous to the analysis of the stability angles in refs. [8].

The instanton path defined in the $2N$-dimensional phase space is $(\bar{\boldsymbol{x}}(t), \bar{\boldsymbol{v}}(t))$ $t \in [0, T]$. (In sect. 3 we have rescaled the coordinates to have unit mass.) Let us take a neighboring classical path, $\boldsymbol{x}'(t) = \bar{\boldsymbol{x}}(t) + \boldsymbol{q}(t)$, which deviates from $(\bar{\boldsymbol{x}}, \bar{\boldsymbol{v}})$ by an infinitesimal fluctuation $(\boldsymbol{q}(t), \boldsymbol{p}(t))$, where $\boldsymbol{p} = \dot{\boldsymbol{q}}$. The gradient of the classical action W with respect to its final (initial) position is equal to the final (negative of initial) momentum. We can thus use the second derivatives of the instanton action $W(\bar{\boldsymbol{x}}^{(1)}, \bar{\boldsymbol{x}}^{(2)}, E)$ to define a transformation on the surface of constant energy E. This is a linear transformation between the coordinate fluctuations $\boldsymbol{q}(0), \boldsymbol{q}(T)$, and the momenta fluctuations $\boldsymbol{p}(0), \boldsymbol{p}(T)$, such that the neighboring paths, defined by these deviations, are constrained to have energy E. In an $(N \times N)$ matrix notation we write this transformation as

$$\begin{aligned} \boldsymbol{p}(0) &= -W^{11} \cdot \boldsymbol{q}(0) - W^{12} \cdot \boldsymbol{q}(T), \\ \boldsymbol{p}(T) &= W^{21} \cdot \boldsymbol{q}(0) + W^{22} \cdot \boldsymbol{q}(T), \end{aligned} \tag{B.1}$$

where

$$W^{\alpha\beta} = \frac{\partial^2}{\partial \boldsymbol{x}^\alpha \, \partial \boldsymbol{x}^\beta} W(\bar{\boldsymbol{x}}^{(1)}, \bar{\boldsymbol{x}}^{(2)}, E). \tag{B.2}$$

We wish to express eq. (B.1) in terms of two coordinate systems which single out the direction of the instanton velocities $\bar{\boldsymbol{v}}(0)$ and $\bar{\boldsymbol{v}}(T)$. Thus we define for any time t

the moving coordinate system $\hat{\eta}_i(t)$, $i = 1, N$, such that

$$\hat{\eta}_1(t) = \frac{\bar{v}(t)}{v(t)}, \qquad v = |\bar{v}|, \tag{B.3a}$$

$$\hat{\eta}_i(t) \cdot \hat{\eta}_j(t) = \delta_{ij}. \tag{B.3b}$$

Henceforth we shall use *Latin subscripts* to denote the components of a matrix along the two endpoint basis vectors, e.g.

$$W_{ij}^{11} = \hat{\eta}_i(0) \cdot W^{11} \cdot \hat{\eta}_j(0), \qquad W_{ij}^{12} = \hat{\eta}_i(0) \cdot W^{12} \cdot \hat{\eta}_j(T), \text{ etc.}, \tag{B.4a}$$

and the fluctuations in the moving frame as

$$q_i(t) = \hat{\eta}_i(t) \cdot \boldsymbol{q}(t), \qquad p_i(t) = \hat{\eta}_i(t) \cdot \boldsymbol{p}(t) \tag{B.4b}$$

(as opposed to the *bold face* notation for vectors in a time-independent representation). By taking the $\boldsymbol{x}'$ derivatives of the hamiltonian

$$H\big(\boldsymbol{x}, \nabla_{\boldsymbol{x}} W(\boldsymbol{x}, \boldsymbol{x}', E)\big) = E, \tag{B.5}$$

and using eq. (B.3a) one can verify that

$$W_{1i}^{12} = W_{i1}^{12} = 0, \qquad i = 1, N. \tag{B.6}$$

We write eq. (B.1) in terms of the $W_{ij}^{\alpha\beta}$ elements. A summation or a determinant with a prime denotes projecting out all the 1-components. We denote by a tilde (e.g. $\tilde{W}_{ij}^{12}$), the minor of a matrix which has its first row and column removed. Let us invert the minors $\tilde{W}^{12}$ and $\tilde{W}^{21}$ in eq. (B.1) and obtain the "area preserving transformation" of the perpendicular fluctuations:

$$q_i(T) = \sum_{j=2}^{N} \tilde{A}_{ij} q_j(0) + \sum_{j=2}^{N} \tilde{B}_{ij} p_j(0), \qquad i = 2, N,$$

$$p_i(T) = \sum_{j=2}^{N} \tilde{C}_{ij} q_j(0) + \sum_{j=2}^{N} \tilde{D}_{ij} p_j(0), \qquad i = 2, N, \tag{B.7}$$

where the matrices $\tilde{A}$, $\tilde{B}$, $\tilde{C}$ and $\tilde{D}$ are given by

$$\tilde{A} = -(\tilde{W}^{12})^{-1} \tilde{W}^{11}, \qquad \tilde{B} = -(\tilde{W}^{12})^{-1},$$

$$\tilde{C} = \tilde{W}^{21} - \tilde{W}^{22}(\tilde{W}^{12})^{-1} \tilde{W}^{11}, \qquad \tilde{D} = -\tilde{W}^{22}(\tilde{W}^{12})^{-1}. \tag{B.8}$$

The equations of motion for the fluctuations are also called the "variational equations of Jacobi or Poincaré" [7] and are derived by linearizing hamilton's equations about the instanton path. In the stationary coordinate representation these are N second-order coupled equations:

$$\ddot{\boldsymbol{q}} = \Omega^2 \cdot \boldsymbol{q}, \qquad \Omega^2 = \frac{\partial^2}{\partial \boldsymbol{x}\, \partial \boldsymbol{x}'} V(\bar{\boldsymbol{x}}(t)). \tag{B.9}$$

The additional constraint we have is fixing the energy E of any deviating path. If H is the hamiltonian, this implies

$$H(\bar{\boldsymbol{x}} + \boldsymbol{q}, \bar{\boldsymbol{v}} + \boldsymbol{p}) - H(\bar{\boldsymbol{x}}, \bar{\boldsymbol{v}}) = 0 = \bar{\boldsymbol{v}}(t) \cdot \boldsymbol{p}(t) - \dot{\bar{\boldsymbol{v}}}(t) \cdot \boldsymbol{q}(t). \tag{B.10}$$

When we write the stability equations, eq. (B.9), in the moving frame, additional terms with $\dot{\hat{\eta}}_i$ and $\ddot{\hat{\eta}}_i$ will enter the equations. These terms represent the "Coriolis forces" which act on the projected transverse fluctuations because of the rotation of the moving frame around $\hat{\eta}_1$. However we shall simplify the equations by choosing a "*parallel transported*" moving frame, i.e. imposing the conditions

$$\dot{\hat{\eta}}_i(t) \cdot \hat{\eta}_j(t) = 0, \qquad i, j = 2, N, \qquad 0 \leqslant t \leqslant T. \tag{B.11}$$

The $N-1$ "bending frequencies"

$$J_{1i}(t) \equiv \dot{\hat{\eta}}_1(t) \cdot \hat{\eta}_i(t), \qquad i = 2, N, \tag{B.12}$$

are thus defined. Eq. (B.10) can be written as

$$v\dot{q}_1 - \dot{v}q_1 - 2v \sum_{i=2,N} J_{1i} q_i = 0. \tag{B.13}$$

After some algebraic manipulations, which use eq. (B.13) to eliminate the functions $q_1(t)$ and $\dot{q}_1(t)$ from the equations for $q_i(t)$, $i \neq 1$, we arrive at the $N-1$ coupled equations

$$\ddot{q}_i(t) = \sum_{i'=2,N} \left[\Omega^2_{ii'}(t) - 3\delta_{ii'}(J_{1i'}(t))^2\right] q_{i'}(t), \qquad i = 2, N. \tag{B.14}$$

Eqs. (B.7) and (B.8) are used to rewrite the semiclassical wave function prefactor Λ_n of eq. (3.25):

$$\begin{aligned}
\Lambda_n &= \left(\frac{v(0)}{v(T)}\right)^{1/2} \left[\frac{\det'|-\tilde{W}^{12}|}{\det'|\tilde{W}^{11}+\phi|}\right]^{-1/2} \\
&= \left(\frac{v(0)}{v(T)}\right)^{1/2} \det' \left| \frac{\partial q_i(T)}{\partial q_j(0)} + \sum_{j'=2,N} \frac{\partial q_{i'}(T)}{\partial p_{j'}(0)} \phi_{j'j} \right|^{-1/2} \\
&= \left(\frac{v(0)}{v(T)}\right)^{1/2} \det'|q_{ij}(T)|^{-1/2},
\end{aligned} \tag{B.15}$$

where q_{ij} are the solutions to eq. (B.14) with the initial conditions

$$q_{ij} = \delta_{ij}, \qquad \dot{q}_{ij} = \phi_{ij}, \qquad i, j = 2, N. \tag{B.16}$$

The prefactor of the tunneling matrix element $\Lambda_{n,n'}$ in eqs. (3.29) can be expressed analogously as

$$\begin{aligned}\Delta_{n,n'} &= \det{}'\left|\tilde{W}^{21} - (\tilde{W}^{12})^{-1}\left[\tilde{W}^{11} + \phi^{(1)}\right]\left[\tilde{W}^{22} + \phi^{(2)}\right]\right|^{-1/2} \\ &\quad \times (v(0)v(T))^{1/2}(2\pi g)^{(N-1)/2} \\ &= \det{}'\left|\dot{q}_{ij}(T) + J_{1i}q_{1j}(T) + \sum_{i'=2,N} \phi^{(2)}_{ii'}q_{i'j}(T)\right|^{-1/2} \\ &\quad \times (v(0)v(T))^{1/2}(2\pi g)^{(N-1)/2},\end{aligned} \tag{B.17}$$

where q_{ij} are the solutions of eqs. (B.14) with initial conditions (B.16) ($\phi \to \phi^{(1)}$), and $q_{1j}(T)$ is obtained simply by integrating eq. (B.13):

$$q_{1j}(T) = 2v(T) \sum_{i'=2,N} \int_0^T \mathrm{d}t \, \frac{J_{1i'}(t)q_{i'j}(t)}{v(t)}. \tag{B.18}$$

Appendix C

THE 2D HARMONIC OSCILLATOR WAVE FUNCTION

Here we show an example of the semiclassical evaluation of the single surface PDX, using the procedure described in subsect. 3.3. We choose the two-dimensional harmonic oscillator as the model problem although its wave functions are known everywhere in the (x, y) plane in an exact form. However, the classical dynamics of the instanton path and the transverse fluctuations around it are non-trivial, since the path is not linear in the two coordinates (it curves as a power law). Thus, working out the semiclassical approximation in this problem would be instructive for understanding the different contributions to the exponent and prefactor also in other potentials. A generalization of this problem to any higher dimension harmonic oscillator is straightforward.

Let us use dimensionless coordinates (x, y), scale the mass to unity, and use g as the quantum parameter (instead of $\hbar$). The potential is

$$V(x, y) = \tfrac{1}{2}\omega_x^2 x^2 + \tfrac{1}{2}\omega_y^2 y^2. \tag{C.1}$$

The energy of the wave function ψ_{nm} is

$$E_{nm} = g\left(n + \tfrac{1}{2}\right)\omega_x + g\left(m + \tfrac{1}{2}\right)\omega_y . \tag{C.2}$$

We follow the prescription of subsect. 3.3 to find the wave function $\psi_{nm}(x^{(2)}, y^{(2)})$ *deep* in the forbidden region ($V(x^{(2)}, y^{(2)}) \gg E_{nm}$), to leading order in g. This procedure is illustrated in fig. 6.

(i) We expand the wave function $\psi_{nm}(x, y)$ to leading order in g, in the forbidden region. Thus, only the leading powers of x and y are kept:

$$\psi_{nm}(x, y) = c_n x^n c_m y^m \exp\left[-\frac{1}{g}\left(\frac{1}{2}\omega_x x^2 + \frac{1}{2}\omega_y y^2\right)\right](1 + \mathrm{O}(g))$$

$$\equiv p_{nm}(x, y)\exp\left[-\frac{1}{g}\phi(x, y)\right](1 + \mathrm{O}(g)), \tag{C.3}$$

thus defining the prefactor p and the exponent ϕ.

(ii) The decomposition surface Σ is chosen to be at

$$\phi_{nm}(x, y) = d \gg 1 . \tag{C.4}$$

d is still much smaller than $\phi_{nm}(x^{(2)}, y^{(2)})$. (The result, of course, will be independent of d.)

(iii) Although the instanton path $(\bar{x}, \bar{y})$ is classical path of energy $-E_{nm}$ in the inverted potential, it is substituted with the path of zero energy which leaves Σ perpendicularly and reaches $(\bar{x}^{(2)}, \bar{y}^{(2)})$ at time T. The first-order correction to the instanton action from the shift of the energy from $-E_{nm}$ to zero, is $E_{nm}T$, which is of order g, and thus we include it in the prefactor eq. (C.7). Since we chose Σ in the forbidden region, the second derivative of the action exists and higher-order corrections in g do not contribute to the semiclassical level of approximation. The instanton path can be parametrized by the time t, so

$$\bar{x}(t) = \bar{x}^{(1)} \mathrm{e}^{\omega_x t}, \qquad \bar{y}(t) = \bar{y}^{(1)} \mathrm{e}^{\omega_y t}, \tag{C.5a}$$

$$v(t) = \sqrt{\left(\omega_x \bar{x}^{(1)} \mathrm{e}^{2\omega_x t}\right)^2 + \left(\omega_y \bar{y}^{(1)} \mathrm{e}^{2\omega_y t}\right)^2}, \tag{C.5b}$$

or by the x-coordinate itself, in which case

$$(\bar{x}, \bar{y}) = (x, \bar{y}(x)), \qquad \bar{y}(x) = \bar{y}^{(1)}\left(x/\bar{x}^{(1)}\right)^{\omega_y/\omega_x}, \tag{C.5c}$$

where $(\bar{x}^{(1)}, \bar{y}^{(1)})$ is the instanton point on Σ.

(iv) The exponential contribution $\tilde{\phi}$ to the wave function at $(x^{(2)}, y^{(2)})$ is the sum of the instanton action and the wave function exponent $\phi(\bar{x}^{(1)}, \bar{y}^{(1)})$, thus we verify that

$$\frac{1}{g}\tilde{\phi}(x^{(2)}, y^{(2)}) = \frac{1}{g}\left[\phi(\bar{x}^{(1)}, \bar{y}^{(1)}) + \int_{\bar{x}^{(1)}}^{x^{(2)}} \mathrm{d}x \sqrt{2V(x, \bar{y}(x))\left(1 + \left(\frac{\mathrm{d}\bar{y}}{\mathrm{d}x}\right)^2\right)}\right]$$

$$= \frac{1}{g}\phi(x^{(2)}, y^{(2)}). \tag{C.6}$$

(v) The prefactor is given using eqs. (3.28):

$$\tilde{p}_{nm}(x^{(2)}, y^{(2)}) = p_{nm}(\bar{x}^{(1)}, \bar{y}^{(1)})\exp\left[\frac{1}{g}E_{nm}T\right]\left(\frac{v(0)}{v(T)q(T)}\right)^{1/2}. \tag{C.7}$$

Where the fluctuation q obeys

$$\ddot{q} = \left[\Omega^2(t) - 3J^2(t)\right]q, \tag{C.8a}$$

with the initial condition

$$q(0) = 1, \tag{C.8b}$$

$$\dot{q}(0) = \frac{1}{(v(0))^2}\left[\omega_y\left(\omega_x\bar{x}^{(1)}\right)^2 + \omega_x\left(\omega_y\bar{y}^{(1)}\right)^2\right], \tag{C.8c}$$

where

$$\Omega^2 = \left[\frac{\omega_x\omega_y}{v(t)}\right]^2\left[\left(\bar{x}^{(1)}\right)^2 e^{2\omega_x t} + \left(\bar{y}^{(1)}\right)^2 e^{2\omega_y t}\right], \tag{C.8d}$$

$$J = \frac{1}{(v(t))^2}\omega_x\omega_y\bar{x}^{(1)}\bar{y}^{(1)}(\omega_x - \omega_y)e^{(\omega_x+\omega_y)t}. \tag{C.8e}$$

The solution to eqs. (C.8) is

$$q(t) = \frac{v(0)}{v(t)}e^{(\omega_x+\omega_y)t}. \tag{C.9}$$

Using eqs. (C.9) and (C.5) in eq. (C.7) we can cancel the T-dependence and verify that indeed

$$\tilde{p}_{nm}(x^{(2)}, y^{(2)}) = p_{nm}(x^{(2)}, y^{(2)}). \tag{C.10}$$

Appendix D

THE ADIABATIC FLUCTUATIONS APPROXIMATION

This appendix briefly treats a special case of tunneling problems in which the prefactor calculation can be simplified a great deal by the use of the adiabatic approximation for the transverse degrees of freedom. (We call this method the "adiabatic fluctuations approximation" (AFA) and we intend to discuss it more fully in a future study.) The transverse coordinates, which are denoted by the vector y, are defined to be perpendicular to the instanton path $\bar{x}(t)$. The AFA is an adiabatic approximation in that it approximates the contribution to the path integral of transverse fluctuations by a local function of the position along the instanton path. The system is thus always in an instantaneous eigenstate with respect to the transverse motion, corresponding to fixed x, and this state is adiabatically transported along the instanton path. This results in a renormalization of the potential along the path by an amount equal to the instantaneous transverse energy eigenvalue. The AFA is clearly valid when the motion along the instanton path is sufficiently slow, in a sense which emerges naturally from the analysis below. We will also discuss what happens in the opposite limit, where the inverse-adiabatic (sudden) approximation can be used.

We will only consider the case in which the instanton path is straight. (We ignore "bending" effects. However, the more general case can be treated in a similar fashion.) For the instanton path to be straight, it is necessary that on the x-axis, the potential $V(x, y)$ has a vanishing gradient in the y-directions. Hence to leading order in y

$$V(x, y) = V_1(x) + \tfrac{1}{2} y \cdot \Omega^2(x) \cdot y + \cdots . \tag{D.1}$$

Here, $\Omega^2(x)$ is the curvature matrix of the potential which has eigenvalues $\Omega_j^2(x)$ and corresponding eigenvectors $\hat{\eta}_j(x)$, $j = 2, N$. We define the x-dependent constrained harmonic oscillator states $\chi_{n_j}(y_j|x)$,

$$\left[-\tfrac{1}{2} g^2 \partial_{y_j}^2 + \tfrac{1}{2} \Omega_j^2(x) y_j^2 \right] \chi_{n_j}(y_j|x) = \varepsilon_{n_j}(x) \chi_{n_j}(y_j|x) , \tag{D.2}$$

where y_j is the component of y along $\hat{\eta}(x)$:

$$y_j = y \cdot \eta_j(x) . \tag{D.3}$$

The PDX expressions for the wave function ψ_n or the tunneling matrix elements $M_{n,n'}$ (eqs. (3.17a) and (2.39) respectively) are evaluated as follows: as always, the decomposition surfaces Σ_i are chosen to be perpendicular to the instanton path (x-axis) at positions $x_d^{(i)}$. The restricted wave functions, whose matrix elements we will calculate, are assumed to be given by the constrained states

$$\psi_{\boldsymbol{n}}^{(i)} = \chi_{n_1}\left(x_d^{(i)}\right) \prod_{j=2}^{N} \chi_{n_j}\left(y_j | x_d^{(i)}\right) , \tag{D.4a}$$

which have eigenenergies

$$E_{\boldsymbol{n}}^{(i)} = \varepsilon_{n_1} + \sum_{j=2}^{N} \varepsilon_{n_j}\left(x_{\mathrm{d}}^{(i)}\right). \tag{D.4b}$$

The transition Green function $G^{\mathrm{tr}}(E)$ (which is $G^{\mathrm{r}}(E)$ in the wave function expression) is the Laplace transform of the transition propagator K^{tr} which we write in imaginary time as

$$K^{\mathrm{tr}}(x, y; x', y', -iT) = \int_{x(0)=x}^{x(T)=x'} \mathcal{D}[x] \mathrm{e}^{-S_1[x]/g} \int_{y(0)=y}^{y(T)=y'} \mathcal{D}[y] \mathrm{e}^{-S_2[x,y]/g}, \tag{D.5a}$$

where

$$S_1 = \int_0^T \mathrm{d}t \left\{ \tfrac{1}{2}\dot{x}^2 + V^{\mathrm{ren}}(x) \right\}, \tag{D.5b}$$

$$S_2 = \int_0^T \mathrm{d}t \left\{ \tfrac{1}{2}\dot{y}^2 + V(x, y) - V^{\mathrm{ren}}(x) \right\}, \tag{D.5c}$$

and $V^{\mathrm{ren}}(x)$ is a potential which depends only on x. We shall eventually choose it to be a suitably renormalized potential:

$$V_{\boldsymbol{n}}^{\mathrm{ren}} = V_1(x) + \bar{\varepsilon}_{\boldsymbol{n}}(x). \tag{D.5d}$$

(The appearance of the vector index $\boldsymbol{n}$ will be explained at that time.) The AFA approximation to K^{tr} yields

$$K^{\mathrm{tr}} = K_1 K_2 \left[1 + \mathrm{O}(g) + \mathrm{O}\left(\sum_j |\alpha_j| \right) \right], \tag{D.6a}$$

where K_1 is only dependent on x, x':

$$K_1 = \sqrt{\det \left| \frac{-1}{2\pi g} \frac{\partial^2 S_1[\bar{x}]}{\partial x \, \partial x'} \right|} \exp\left[-\frac{1}{g} S_1[\bar{x}] \right], \tag{D.6b}$$

$\bar{x}$ is the classical path in the renormalized potential, and

$$K_2(y, y', \{\bar{x}(t)\}, -iT) = \prod_{j=2}^{N} \left\{ \sum_{n_j=0}^{\infty} \chi_{n_j}(y_j|x) \chi_{n_j}(y_j'|x') \right\} \times \exp\left[-\frac{1}{g} \int_0^T \mathrm{d}t \left[\left\{ \sum_{j=2}^{N} \varepsilon_{n_j}(\bar{x}) \right\} - \bar{\varepsilon}_n(\bar{x}) \right] \right]. \tag{D.6c}$$

Eq. (D.6) is arrived at using three separate approximations: firstly, we apply the semiclassical approximation, and express the path integral in eq. (D.5a) in terms of the classical path between the endpoints (x, y) and (x', y'). Secondly, we expand the action of this path to quadratic order in the transverse endpoints y and y' and obtain the expression for K_2 as

$$K_2(y, y', \{\bar{x}(t)\}, -iT) = \det\left|\frac{-1}{2\pi g}\frac{\partial^2 S_2}{\partial y\,\partial y'}\right|^{1/2}_{y-y'=0} \times \exp\left[-\frac{1}{g}\left[S_2(y, y', \{\bar{x}\}, T) - \int_0^T \mathrm{d}t\,\bar{\varepsilon}_n(\bar{x})\right]\right], \tag{D.7a}$$

where

$$S_2[y, y', \{\bar{x}\}, T] = \tfrac{1}{2}\sum_{j=2}^{N}\left\{\dot{\bar{y}}_j(T)\,y_j' - \dot{\bar{y}}_j(0)\,y_j\right\}, \tag{D.7b}$$

where $\bar{y}_j(t)$ are the perpendicular components of the classical paths with the given endpoints at y and y'. Lastly, we evaluate eqs. (D.7) by solving the *classical* dynamics of the $\bar{y}_j(t)$ coordinates in the adiabatic approximation. The linearized equations of motion for these coordinates are the same as the transverse fluctuation equations eqs. (3.27) but with *endpoint* boundary conditions instead of initial conditions. (Note, since by assumption the instanton path is straight, the bending frequencies in eqs. (3.27) are zero.) This implies that each coordinate $\bar{y}_j(t)$ is approximated by the adiabatic solution

$$\bar{y}_j(t) = \frac{1}{\sinh\left[\int_0^T \mathrm{d}t\,\Omega_j\right]}\left\{y_j\sqrt{\frac{\Omega_j(0)}{\Omega_j(t)}}\sinh\left[\int_t^T \mathrm{d}t\,\Omega_j\right] + y_j'\sqrt{\frac{\Omega_j(T)}{\Omega_j(t)}}\sinh\left[\int_0^T \mathrm{d}t\,\Omega_j\right]\right\} \times\left[1 + \mathrm{O}(\alpha_j)\right], \tag{D.8}$$

where the α_j's are the small adiabaticity parameters of the approximation

$$\alpha = \langle \dot{\Omega}_j/\Omega_j^2\rangle \ll 1. \tag{D.9}$$

$\langle\ \rangle$ denotes "typical-value-of" along the instanton path. The sum over constrained states in (D.6c) is derived in a manner which is analogous to Feynman and Hibbs [4] derivation of the harmonic oscillator eigenstates from its propagator. (It is the result of expanding K_2 in powers of $\exp[-\int \mathrm{d}t\,\Omega_j]$.)

Because the wave function $\psi_n^{(i)}$ has the form of (D.4a), the particular set of quantum numbers $\boldsymbol{n} = n_2, n_3, \ldots n_N$ will be projected out of K_2 once the surface integrals have been performed. Thus, we can choose $\bar{\varepsilon}_n(x)$, so that all the exponential dependence of K on the path $\bar{x}(t)$ appears in K_1:

$$\bar{\varepsilon}_n(x) = \sum_{j=2}^{N} \varepsilon_{n_j}(x). \tag{D.10}$$

The renormalization of the instanton action simplifies the expression for $G^{\mathrm{tr}}(E)$ and subsequently the wave function or transition matrix elements calculation. As an example, we work out the AFA solution for the symmetric double well problem. We choose the decomposition surfaces at $\pm x_{\mathrm{d}}$, and the energy $E = E_n^{(1)}$, given by eq. (D.4b). The resulting expression for the tunneling matrix elements is

$$M_{n,n'}(E_n) = |\chi_{n_1}(x_{\mathrm{d}})|^2 v(x_{\mathrm{d}}) \exp\left[-\frac{1}{g} W_n^{\mathrm{ren}}\right] \prod_{j=2}^{N} \delta_{n_j, n'_j}, \tag{D.11a}$$

where

$$W_n^{\mathrm{ren}} = \int_{-x_{\mathrm{d}}}^{x_{\mathrm{d}}} \mathrm{d}x \sqrt{2\left(V_n^{\mathrm{ren}} - E_n^{(1)}\right)}\,. \tag{D.11b}$$

Note that the use of the AFA is limited to cases where α_j are small, the instanton path does not bend rapidly, nor do the transverse eigenvectors $\hat{\eta}_j(x)$ rotate rapidly around the instanton path. In appendix C, the two-dimensional harmonic oscillator wave function calculation provides the converse example of a case where the AFA can fail badly. Here, if the two frequencies are markedly different, then except near a principle axis the instanton paths curve in the $x-y$ plane and the transverse curvatures vary rapidly. In cases where α_j is large only locally in x, i.e. the transverse frequency changes abruptly from, say, $\Omega_1 = \Omega(a-\delta)$ to $\Omega_2 = \Omega(a+\delta)$, for small δ, the sudden approximation can be applied in conjunction with the AFA. This yields additional overlap factors P_{m_j, m'_j} in K_2 of eq. (D.6c):

$$P_{m_j, m'_j} = \int \mathrm{d}y_j \chi_{m_j}(y_j|a-\delta)\chi_{m'_j}(y_j|a+\delta) \leqslant 1. \tag{D.12}$$

We conclude by noting that this approximation can be generalized to cases where the potential cannot be expanded as a quadratic function of y as in eq. (D.1). The generalization simply amounts to replacing the states χ_{n_j} and ε_{n_j} by the appropriate constrained eigenstates and energies. (An example is the case when the transverse potential is a square well. In an analogous problem in classical electrodynamics, the low-frequency standing-waves of two microwave resonators weakly coupled by a narrow wave guide are analogous to the low-lying states of the same quantum square double-well.)

References

[1] A. Auerbach, S. Kivelson and D. Nicole, Phys. Rev. Lett. 53 (1984) 411; (E) 53 (1984) 2275
[2] E. Merzbacher, Quantum mechanics (Wiley, New York, 1961) ch. 7
[3] J. Sethna, Phys. Rev. B24 (1981) 698
[4] R.P. Feynman and A.R. Hibbs, Quantum mechanics and path integrals, (McGraw-Hill, New York, 1965)
[5] L.S. Schulman, Techniques and applications in path integration (Wiley, New York, 1981)
[6] A. Auerbach and L.S. Schulman, A path decomposition expansion proof for the method of images, SUNY, Stony-Brook, NY preprint
[7] L.A. Pars, A treatise on analytical dynamics (Heinemann, London, 1965) 453
[8] M.C. Gutzwiller, J. Math. Phys. 12 (1971) 343;
This analysis was extended to field theories by R. Dashen, B. Hasslacher and A. Neveu, Phys. Rev. D10 (1974) 4114
[9] T. Holstein, Ann. of Phys. 8 (1959) 343
[10] S. Chakravarty and A.J. Leggett, Phys. Rev. Lett. 52 (1984) 5
[11] C.P. Flynn and A.M. Stoneham, Phys. Rev. B1 (1970) 3966
[12] P.W. Anderson, B.I. Halperin and C.M. Varma, Phil. Mag. 25 (1972) 1
[13] S. Goldstein, Proc. R. Soc. (Edinburgh) T49 (1929) 210, sect. III, eq. (2)
[14] H. Goldstein, Classical mechanics (Addison-Wesley, 1980) sect. 8-6
[15] S. Coleman and E. Weinberg, Phys. Rev. D7 (1973) 1888
[16] A. Auerbach, S. Kivelson and A. Zangwill, work in progress
[17] T. Banks, C.M. Bender and T.T. Wu, Phys. Rev. D8 (1973) 3346;
T. Banks and C.M. Bender, Phys. Rev. D8 (1973) 3366
[18] J.S. Langer, Ann. of Phys. 41 (1967) 108
[19] C.G. Callan, Jr. and S. Coleman, Phys. Rev. D16 (1977) 1762;
S. Coleman, The whys of subnuclear physics, ed. A. Zichichi (Plenum, New York, 1977)
[20] R.D. Carlitz and D.A. Nicole, University of Pittsburgh preprint PITT-16-84 (1984), Ann. Phys., to appear
[21] L.D. Chang and S. Chakravarty, Phys. Rev. B29 (1984) 130
[22] A.D. Caldeira and A.J. Leggett, Ann. Phys. 149 (1983) 374
[23] S. Chakravarty and S. Kivelson, Phys. Rev. Lett. 50 (1983) 1811 and Phys. Rev. B32 (1985) 76
[24] S. Chakravarty, Phys. Rev. Lett. 49 (1982) 681
[25] J. Sethna and S. Kivelson, Phys. Rev. B26 (1982) 3513
[26] H. Takayama, Y.R. Lin-Liu and K. Maki, Phys. Rev. B21 (1980) 2388
[27] G.B. Blanchet, C.R. Fincher and A.J. Heeger, Phys. Rev. Lett. 51 (1983) 2132
[28] R. DiFoggio and R. Gomer, Phys. Rev. B25 (1982) 3490;
K.A. Muttalib and J. Sethna, Phys. Rev. B, to be published
[29] P. van-Baal, The energy of electric flux on the hypertorus, ITP, SUNY, Stony-Brook, NY, to be published
[30] A. Auerbach and P. van Baal, Transverse fluctuations in multidimensional tunneling; non-adiabatic effects and induced potentials", preprint ITP-SB-85-28, Stony Brook, NY, to be published
[31] B. Simon, Ann. of Math. 120 (1984) 89